



HAL
open science

Development in the European flounder (*Platichthys flesus*) of a q-PCR assay for the measurement of telomere length, a potential biomarker of pollutant effects for biomonitoring studies

F. Akcha, C. Cahuc, J. Rouxel, C. Munsch, Y. Aminot, T. Chauvelon, K. Mahe, H. Budzinski, A. Mauffret

► To cite this version:

F. Akcha, C. Cahuc, J. Rouxel, C. Munsch, Y. Aminot, et al.. Development in the European flounder (*Platichthys flesus*) of a q-PCR assay for the measurement of telomere length, a potential biomarker of pollutant effects for biomonitoring studies. *Marine Pollution Bulletin*, 2021, 170, pp.112610. 10.1016/j.marpolbul.2021.112610 . hal-03272790

HAL Id: hal-03272790

<https://hal.science/hal-03272790>

Submitted on 30 Apr 2023

HAL is a multi-disciplinary open access archive for the deposit and dissemination of scientific research documents, whether they are published or not. The documents may come from teaching and research institutions in France or abroad, or from public or private research centers.

L'archive ouverte pluridisciplinaire **HAL**, est destinée au dépôt et à la diffusion de documents scientifiques de niveau recherche, publiés ou non, émanant des établissements d'enseignement et de recherche français ou étrangers, des laboratoires publics ou privés.

Development in the European flounder (*Platichthys flesus*) of a q-PCR assay for the measurement of telomere length, a potential biomarker of pollutant effects for biomonitoring studies

Akcha Farida ^{1,*}, Cahuc C. ¹, Rouxe Julien ¹, Munsch Catherine ¹, Aminot Yann ¹,
Chouvelon Tiphaine ¹, Mahe Kelig ², Budzinski H. ³, Mauffret Aourell ¹

¹ Ifremer, Biogeochemistry and Ecotoxicology Research Unit, Nantes, France

² Ifremer, Laboratory of Fisheries Resources, Boulogne-Sur-Mer, France

³ UMR CNRS 5805 EPOC, Laboratory of Physico- and Toxicology of the Environment, Bordeaux, France

* Corresponding author : Farida Akcha, email address : Farida.Akcha@ifremer.fr

Abstract :

Telomeres protect the coding sequence of chromosome ends and Telomere Length (TL) has been proposed as a biomarker of cellular aging, cumulative stress exposure and life-span in humans. With the aim to propose new biomarkers, a q-PCR protocol was adapted for the measurement of TL in the European flounder *Platichthys flesus*. The protocol was then applied in 2-year-old flounders from the Seine Estuary.

The absolute TL in the flounder is 54 ± 13 kbp per genome (mean \pm standard error). Considering relative or absolute TL, no correlation was observed with DNA damage and any of the measured contaminant concentrations (trace elements, metabolites of polycyclic aromatic hydrocarbons, polychlorobiphenyls, organochlorinated pesticides, polybrominated diphenyl ethers, perfluoroalkyl substances). Because sampling was limited, further investigations are required to state a possible impact of chemical pollution on flatfish telomeres. This is motivated by correlations observed with organochlorinated compounds when decreasing statistical significance ($p \leq 0.10$).

Highlights

► A q-PCR protocol was adapted for telomere length (TL) measurement in flounders. ► In fish from Seine Estuary, the absolute TL is 55 ± 12.8 kbp per diploid genome. ► No correlation between TL and DNA damage was observed. ► TL is positively correlated with organochlorinated compounds for p -values ≤ 0.10 . ► More studies are required to state if TL could be a marker of chemical stress.

Keywords : Flatfish, Pollution, Biomonitoring, Telomere, Genotoxicity, DNA damage

30 1. Introduction

1
2 31 Estuarine and coastal marine systems are some of the most fertile ecosystems. They are, however,
3
4 32 exposed to high anthropic pressures, receiving complex mixtures of chemical contaminants from
5
6 33 multiple point and non-point sources. In addition to historical chemical contaminants, such as
7
8 34 polycyclic aromatic hydrocarbons (PAHs) and polychlorobiphenyls (PCBs), in the last decades, the
9
10 35 presence of contaminants of emerging concern (CECs) has attracted growing interest due to the risk
11
12 36 they represent for human and environmental health (Lei et al., 2015). The transfer of chemical
13
14 37 substances is particularly important along the land-sea continuum. Chemical pollution represents a
15
16 38 risk to the biodiversity and the functioning of marine ecosystems. Following absorption and, in some
17
18 39 cases, biotransformation, chemical pollutants can in fact be responsible for various adverse biological
19
20 40 effects.

21 41 Chemical pollution of aquatic ecosystems raises important environmental, sanitary and socio-
22
23 42 economic issues, and an increased awareness has led to changes in European water policies. The Water
24
25 43 Framework Directive (2000/60/EC and 2013/39/EC) and the Marine Strategy Framework Directive
26
27 44 (MSFD 2008/56/EC) aim to achieve a good quality status in member states' water bodies, in particular
28
29 45 by reducing their chemical contamination. Within the MSFD, the anthropic pressure is evaluated by
30
31 46 the assessment of 11 descriptors, of which Descriptor 8 (D8) "Concentrations of contaminants are at
32
33 47 levels not giving rise to pollution effects" especially addresses chemical pollution effects. In France, the
34
35 48 application of MSFD for D8 has led to the implementation of monitoring programmes in the various
36
37 49 marine sub-regions concerned by the metropolitan limits of French marine territory. A list of chemical
38
39 50 contaminants to be measured in abiotic and biotic matrices has been established, including several
40
41 51 trace elements (Ag, As, Cd, Co, Cr, Cu, Fe, Hg, Mn, Mo, Ni, Pb, Zn) and organic contaminants (PAHs,
42
43 52 PCBs, organochlorinated pesticides (OCPs), polybrominated diphenyl ethers (PBDEs) and
44
45 53 perfluoroalkyl substances (PFASs)). In addition, pollutant effects are studied by measuring several
46
47 54 biomarkers in marine organisms (e.g. DNA strand breaks, acetylcholinesterase activity and lysosomal
48
49 55 membrane stability in fish and bivalves). Since 2015, different sites in France have been monitored,
50
51 56 including the highly anthropised Seine Estuary.

52 57 In ecotoxicology, damages to the genetic material are particularly studied. Genotoxicity is a kind of
53
54 58 toxicity shared by a high number of pollutant families, occurring at low exposure levels. It can lead to
55
56 59 negative health effects such as those observed on embryo-larval development and reproduction in
57
58 60 bivalve molluscs and crustaceans (Wessel et al., 2007, Lacaze et al., 2011). Moreover, damage can be
59
60 61 transmitted over generations, leading to multi-and trans-generational effects (Barranger et al., 2014).
62
63 62 Among pollutant-induced DNA lesions, DNA adducts, DNA strand breaks and micronuclei have been

63 widely measured as genotoxicity biomarkers in sentinel flatfish species such as the European flounder,
64 *Platichthys flesus* (Akcha et al. 2003, Hylland 2017). In the Seine Estuary, their measurement in dab
65 *Limanda limanda* showed evidence for fish exposure to genotoxic pollutants such as PAHs (Akcha et
66 al., 2003, 2004, Devier et al., 2013). These genotoxicity biomarkers are on the list of endpoints
67 proposed by the International Council for the Exploration of the Sea (ICES) for an integrated framework
68 to assess chemical pollution in the marine environment.

69 With the aim to pursue the development of genotoxicity biomarkers, it appeared valuable to
70 investigate the impact of chemical pollution on a part of the chromosome structure, the telomeres, in
71 flatfish, poorly investigated until now in ecotoxicology. Telomeres play a key role in maintaining
72 genomic stability by protecting the coding sequence of chromosome ends (Monaghan et al., 2018).
73 Highly conserved across eukaryotes, telomeres are made of tandem repeat of a non-coding short
74 hexameric DNA sequence (TTAGGG). They range from a few to 15 kb in length in humans (Barnes et
75 al., 2019), being even higher (> 30 kp) in several vertebrate animal species (Whittemore et al., 2019).
76 Because of the impossibility to complete DNA replication up to chromosome ends and semi-
77 conservative replication of the DNA, at each cell division, a portion of telomeres is not replicated, and
78 therefore, they are naturally shortened during aging. In humans, telomere length (TL) has been
79 proposed as a potential biomarker of cellular aging and cumulative stress exposure, as well as a
80 prognostic indicator for risk of late-life diseases (Von Zglinicki, 2002). In the last decades, several
81 epidemiology and toxicology studies have highlighted a disruption of telomere dynamics during
82 exposure to oxidative stress as well as physical and chemical agents (Barnes et al., 2018, Moller et al.
83 2018).

84 This seems to be also the case in animals such as birds. In a previous *in-situ* study on the relationship
85 between contaminant exposure and TL in the black-legged kittiwake *Rissa tridactyla* different findings
86 were obtained. In adult females, the TL of red blood cells (RBCs) was negatively correlated with the
87 concentration of an organochlorine pesticide, namely oxychlorane, in the blood (Blévin et al., 2016).
88 In contrast, a positive and significant relationship was observed between PFAS concentration and
89 telomere dynamics in birds presenting higher levels of contamination (Blévin et al., 2017). In fish, a
90 study conducted in the gold fish *Carassius auratus* showed an increase in the level of DNA strand breaks
91 in telomeric regions following exposure to the organophosphorus pesticide monocrotophos,
92 suggesting a potential impact on their length (Zhao et al., 2015). Very recently, shorter telomeres were
93 associated with high levels of phthalate metabolites in the European chub *Squalius cephalus* from
94 urban and agricultural rivers (Molbert et al., 2021). Knowledge on telomeres dynamics in fish is limited;
95 TL length varies from 2 to 25 kb, depending on the species (Ocalewicz, 2013). Unlike in humans,
96 telomerase in fish can be expressed in most tissues throughout the life of the organism (Horn et al.,

97 2008), and a decrease in length over the course of life has not been verified in all fish species (Simide
1 98 et al., 2016).

3
4 99 In the present study, a q-PCR (quantitative Polymerase Chain Reaction) protocol was adapted from
5
6 100 O'Callaghan et al. (2008) for the measurement of relative and absolute TL in the blood of flounders.
7
8 101 The protocol was developed and validated using a composite DNA sample from fish sampled in the
9
10 102 Seine Estuary. To start investigating a possible link between pollution and genome integrity in marine
11
12 103 flatfish, it was then applied in individuals from the same ontogenetic stage. The relationship between
13
14 104 TL, DNA damage (level of DNA strand breaks in the erythrocytes) and chemical body burden (biliary
15
16 105 PAH metabolites, hepatic concentrations in several trace metal elements and muscle concentrations
17
18 106 of mercury, PCBs, PBDEs, OCPs and PFCAS) was investigated.

19 20 21 108 **2. Material and methods**

22 23 109 **2.1 Chemicals**

24
25 110 We purchased NaCl, trizma base, dimethyl sulfoxide (DMSO), normal and low-melting-point agarose,
26
27 111 Triton X-100, foetal calf serum and GelRed from Sigma Aldrich Chemicals. The DNeasy®- Blood and
28
29 112 Tissue kit was obtained from Qiagen, and *E. coli* pUC 19 plasmid, DH5alpha *Escherichia coli* bacteria,
30
31 113 SOC medium, Luria Broth medium and ampicillin were purchased from Thermo fisher Scientific.
32
33 114 PureLink Quick Plasmid DNA Miniprep Kits, purifying DNA with a centrifuge, were obtained from
34
35 115 Invitrogen. Brilliant III Ultra-fast SYBR Green QPCR Master Mix and ROX were purchased from Agilent.
36
37 116 Custom primers and oligomers (84-mer telomeric oligomer and 76-mer GAPDH oligomer) were
38
39 117 synthesised by Eurogentec. Contaminant analyses were conducted using carefully chosen chemicals
40
41 118 selected to satisfy trace analysis requirements. Details can be found in Munsch et al. (2020a) for
42
43 119 organic contaminant analyses in fish tissue. The hydroxy-PAHs and their deuterated homologs were
44
45 120 obtained from Cambridge Isotope Laboratories (Cluzeau Info Labo, Sainte Foy la Grande, France). All
46
47 121 the standards were of analytical grade (> 98%). All the solvents used were of analytical grade (purity >
48
49 122 98%). Dichloromethane and HPLC grade methanol were obtained from Atlantic Labo (Bruges, France).
50
51 123 Deionised water was obtained with a Milli-Q system from Millipore (Molsheim, France).

52 53 125 **2.2 Sampling**

54
55 126 Fish were collected in the Seine Estuary, which is located in the Eastern Channel (Figure 1). It is the
56
57 127 third-largest French estuary (Flipo et al., 2020). It accounts for 50% of the French river transport, and
58
59 128 its catchment area supports 40% of the French economic activity. It is considered to be one of the most
60
61 129 polluted estuaries in Europe (Tappin and Millward, 2015, Burgeot et al., 2017), affected by both large
62
63 130 urban centres (e.g. Paris and its suburbs), wastewater treatment plants, intense industrial (e.g. harbour
64
65

131 and petrochemical activities) and agricultural (mass production of cereal and industrial crops)
132 activities. Nutrients and several contaminants from urban, industrial and agricultural activities are thus
133 discharged into the English Channel by the Seine, the main river flow into the Channel. Species living
134 in the Seine Estuary and the Seine Bay are thus exposed to cocktails of contaminants.

135 Flounders were caught in September 2018 by trawling on the R/V Antéa in the Seine Bay. The sampling
136 was performed during the SELISEINE survey (<https://doi.org/10.17600/18000585>), which is part of the
137 national monitoring survey of the chemical effect (SELI: <https://doi.org/10.18142/285>). The Seine Bay
138 has been previously studied for biomonitoring surveys using dab (Akcha et al. 2003, 2004, Munsch et
139 al. 2004). For the present study, we focused on a sampling area close to the mouth of the Seine Estuary
140 and consequently exposed to the Seine River plume, which carries diverse chemical contaminants.
141 Fish were collected with a small-mesh bottom trawl net. Trawling was limited to 20 min at a speed of
142 3 knots to allow live fish recovery. Only fish having a total length of around 25 cm were selected. This
143 fish length corresponds to 2–3-year-old individuals that are sexually mature (Drevs et al., 1999, van
144 der Hammen and Poos, 2012). They were kept alive on board in a fish well and dissected at the quay.
145 A total amount of 22 fish was available for the study.

146 **2.3 Biometry, collection and storage conditions of individual fish blood, tissues and otoliths**

147 Back to the dock (between 2 and 8 h after fishing), individuals were measured (total length, to the
148 nearest tenth of a cm) and weighed before blood was sampled directly from the caudal vein, using a
149 heparinised syringe. An average of 100 µL of blood was recovered in a cryotube containing RPMI 1640
150 medium supplemented with foetal calf serum (25%) and dimethyl sulfoxide (DMSO; 20%) and stored
151 in liquid nitrogen prior to analysis by the alkaline comet assay for the measurement of DNA stand
152 breaks. The rest was used to isolate total blood cells by centrifugation before storage in liquid nitrogen;
153 these samples were used for the methodological development for TL measurement by q-PCR. Fish
154 were then sacrificed for dissection.

155 Macroscopic observation of the gonads allowed sex determination. The gall bladder was sampled
156 individually for the measurement of biliary hydroxylated PAH metabolites (3-OH BaP, 9-OH BaP, 3-OH
157 Fluo, 1-OH Pyr). The liver was stored below 20°C in acid-cleaned glass vials for trace metal analysis
158 (refer to 2.8). The eviscerated fish was then weighted and saved in a calcined aluminium foil at -20°C
159 prior to dissection of fish muscle under a laboratory hood for subsequent analysis of organic
160 contaminants (PCBs, PBDEs, HBCDDs, OCPs, PFASs) (refer to 2.9) and mercury analysis on this tissue
161 (refer to 2.8). At this final time, sagittal otoliths were collected from the inner ear of each fish (Figure
162 2), cleaned with distilled water and stored at room temperature.

165 **2.4 Otolith sclerochronology**

166 An otolithometric approach was used to determine the age of the 22 flounders according to the
167 international ageing protocol (Vitale et al., 2019). Otoliths (literally ‘earstones’) are paired, calcified
168 pieces of the inner ear of teleosts, growing continuously during fish life and forming annual increments
169 (Panfili et al., 2002). The otolith shape is species-dependent, and for this reason, the ageing
170 preparation could be different among different flatfish species. For flounder, the whole otolith was
171 used. All otoliths were photographed using a ZEISS microscope under transmitted light, assisted by an
172 image analysis system using the TNPC software for digital processing of calcified structures. These
173 calibrated images showed an alternate succession of translucent and opaque bands. It was assumed
174 that the growth annual ring (named “annulus”) consisted of one opaque and one translucent band.
175 Two readers to limit the bias due to ageing analysed each otolith (Vitale et al., 2019).

176

177 **2.5 Development of a q-PCR protocol for the measurement of absolute and relative TL in the**
178 **European flounder**

179 2.5.1 Methodological principles

180 It is noteworthy that due to important chromosomal rearrangements over the course of evolution,
181 some flatfish species may have also telomeres in the body of the chromosomes, so-called “ITS”
182 (interstitial telomere sequences), which are mostly shorter than telomeres (Bitencourt et al., 2014).
183 Because the Senegalese sole *Solea senegalensis* and the Atlantic halibut *Hippoglossus hippoglossus* are
184 ITS-free (Ocalewicz et al., 2008 and Cross et al., 2006), this is expected to be also the case in the
185 flounder, which belongs to the same phylogenetic *Pleuronectidae* family. Therefore, there is no risk of
186 underestimating telomere length in these sentinel species due to the presence of ITS (Foote et al.,
187 2013).

188 The use of the Terminal Restriction Fragment (TRF) is the reference method to measure TL (Harley et
189 al., 1990). Because it requires less DNA quantity, q-PCR was first used by Cawthon et al. (2002) to
190 measure the relative TL in human RBCs by establishing the ratio between the cycle threshold value (Ct)
191 of the telomeric sequence (T) and those of a single-copy reference gene (S). The q-PCR has been widely
192 applied, and in 2008, O’Callaghan et al. proposed an advanced q-PCR protocol for the measurement of
193 both relative and absolute TL. The authors generated an external calibration curve based on the
194 amplification of known quantities of a telomeric oligomer of a known base pair number. A similar
195 calibration curve was also obtained for a single-copy reference gene to allow the determination of the
196 number of genome copies present in the samples. With these curves, it was thus possible to give a
197 value for absolute TL in kilobase pair (kbp) per unit of genome present in each sample subjected to
198 amplification.

199

200 2.5.2 DNA extraction

1 201 The DNA was extracted from flounder blood cells using the DNeasy®-Blood and Tissue kit, following
2
3 202 the recommendations of the manufacturer. Once extracted, DNA concentration and quality were
4
5 203 measured by spectrophotometry at 230, 260 and 280 nm, using a Nanodrop ND1000. The DNA samples
6
7 204 presenting 260/280 and 260/230 ratios, around 1.8 and 2, respectively, were considered as pure. For
8
9 205 the quantification, one optic density unit at 260 nm corresponded to a concentration of 50 µg pure
10
11 206 DNA per mL.

12 207

14 208 2.5.3 Plasmid DNA extraction

15 209 For TL measurement by qPCR, it is recommended to maintain the initial DNA quantity constant for the
16
17 210 establishment of standard calibration curves (O'Callaghan et al., 2008). To do so, plasmid DNA deprived
18
19 211 of the telomeric sequence was used. First, 2 µL of *E. coli* pUC 19 plasmid were added to 100 µL of
20
21 212 DH5alpha *E. coli* bacteria, and plasmid insertion was realised by thermal shock (30 s at 42°C, followed
22
23 213 by a rapid switch into the ice to tighten pores and to entrap plasmids inside the cells). Bacteria were
24
25 214 then incubated with SOC medium (tryptone 2%, yeast extract 0,5%, NaCl 10mM, KCl 2,5 mM, MgCl₂
26
27 215 10mM, MgSO₄ 10 mM, glucose 20mM) for at least 30 min to allow cell transformation. Subsequently,
28
29 216 they were cultured in a petri dish containing ampicillin-enriched Luria Broth (LB) medium for 24 hrs at
30
31 217 37°C. In these conditions, only bacteria with inserted plasmid DNA expressed the ampicillin resistance
32
33 218 trait phenotype. Those bacteria were then recovered and suspended in ampicillin-enriched LB medium
34
35 219 for 24 h at 37°C prior to DNA extraction using the "Pure Link Quick Plasmid DNA Miniprep Kits- Purifying
36
37 220 DNA with a centrifuge", following the manufacturer's instructions. Plasmid DNA concentration and
38
39 221 quality were determined as previously described.

40 222

41 223 2.5.4 q-PCR assay

42 224 We performed q-PCR using the Brilliant III Ultra-fast SYBR Green QPCR Master Mix kit, following the
43
44 225 manufacturer's instructions. The adaptation of the protocol from O'Callaghan et al. (2018) was realised
45
46 226 using a composite DNA sample made of genetic material from the different fish caught at ES station.
47
48 227 The use of a kit was not conducive to modifications on Taq polymerase quantity and composition and
49
50 228 quantity of the reaction buffer. Four parameters of the qPCR procedure were tested to optimise
51
52 229 sensibility and specificity of the telomere length measurement in flounder: the quantity of amplified
53
54 230 DNA (7.8×10^{-2} to 5 ng), the primer set (refer to 2.6.4.1), the hybridisation temperature (54 to 60°C)
55
56 231 and the ratio of forward and reverse primers (1 to 3); those values were chosen according either to
57
58 232 previous published protocols (Cawthron et al., 2002, O'Callaghan et al., 2008, Angelier et al., 2013) or
59
60 233 to the manufacturer's recommendations.

269 The q-PCR assays were run using the Stratagene MX3000P instrument with the Stratagene MXPro
1 270 software. Telomere and GAPDH were amplified for each fish sample on two different polypropylene
2 271 96-well tube plates. On each plate, the corresponding oligomer was also run to generate the external
3 272 calibration curve. A No Template Control (water and reaction mix only) and a composite sample of fish
4 273 DNA were also analysed on each plate to check for contamination and inter-plate variation,
5 274 respectively.

10 275 The QPCR Master Mix contained the mutant Taq DNA polymerase, dNTPs, Mg²⁺, a buffer specially
11 276 formulated for fast cycling and the double-stranded DNA-binding dye SYBR Green I for detection
12 277 (excitation and emission wavelengths of 254 and 520 nm, respectively). The forward and reverse
13 278 primers (see 2.6.3.1) and a reference dye (ROX at 1:500, 30 nM) were then added into the mix and
14 279 gently mixed. The passive reference dye is included in the kit to compensate for non-PCR-related
15 280 variations in fluorescence, providing a stable baseline to which samples are normalised (excitation and
16 281 emission wavelengths of 584 and 612 nm, respectively). After distributing the mix in the plate's well,
17 282 1 ng of DNA was added per reaction (plasmid DNA was used to maintain the amount constant); the
18 283 final total reaction volume was 20 µL. The plate was then homogenised and centrifuged. For both
19 284 telomeres and single-copy gene, PCR conditions were as follows: 3 min at 95°C (Taq activation), 40
20 285 cycles of 20s at 95°C, followed by 20s at 60°C (denaturation of dsDNA template followed by annealing
21 286 and extension of the primers), 95°C for one min, 30s at 55°C, 30s at 95°C (dissociation step). Regarding
22 287 the calibration point, each fish sample was run in triplicate, and some samples were run a second time
23 288 when the difference in Ct values among the triplicates was greater than 1 Ct.
24 289

290 2.5.4.4 Calculation of relative and absolute TL

37 291 The relative TL was determined as described by Cawthon et al. (2002) by the ratio between the Ct value
38 292 of the telomeric sequence (T) and that of a single-copy reference gene (S).

42 293 The absolute TL was determined based on the calibration curves obtained for the telomeric sequence
43 294 and the reference gene, as described by O'Callaghan et al. (2008). The oligomer standard for the
44 295 telomeres has a molecular weight (MW) of 26,667.2
45 296 (<http://biotools.nubic.northwestern.edu/OligoCalc.html>). The weight of one molecule (the Avogadro's
46 297 number gives the number of units in a mole) was therefore 0.44×10^{-19} g for a 84-mer length. For each
47 298 amplified quantity of the oligomer standard, it is therefore possible to assign a number of total
48 299 amplified TL in kilobase pairs to each Ct value. Concerning the reference gene, the weight of one
49 300 amplicon molecule was calculated (MW/Avogadro's number) and used to determine the number of
50 301 diploid genome copies present in amplified DNA (quantity of standard divided by the amplicon weight
51 302 and then by 2 to take into account diploidy). By using these calibration curves, the absolute TL of each
52 303 fish DNA sample was determined and expressed in kbp/diploid genome.

304

1 305 **2.6 Investigating *in situ* the relationship between chemical pollution and genome integrity in**
2
3 306 **flounder**

4
5 307

6
7 308 Because age can have an influence on TL, it was decided to focus on 2-year-old fish, representing most
8
9 309 of the fish collected at ES during the survey (see 3.1). TL, DNA damage and complete chemical analysis
10
11 310 were conducted on the same set of samples made of 8 fish (4 males and 4 females).

12 311

13
14 312 **2.6.1 Measurement of DNA strand breaks in fish erythrocytes**

15
16 313 The comet assay was applied as previously described (Akcha et al., 2003). Two comet slides were
17
18 314 prepared per blood sample; DNA unwinding and electrophoresis (390 mA, $E = 0.66 \text{ V cm}^{-1}$) duration
19
20 315 were, respectively, 15 and 20 min. To obtain permanent preparations, the slides were immersed for
21
22 316 10 min in absolute ethanol for dehydrating and allowed to dry at room temperature. Immediately prior
23
24 317 to analysis, 75 μL of GelRed at 8 mg L^{-1} were spread over each slide using a cover glass. The slides were
25
26 318 placed for at least 1 h in the dark at 4°C for coloration and then analysed using an optical fluorescence
27
28 319 microscope (Olympus BX60 $\times 40$) equipped with a CDD camera (Luca-S, Andor Technology) and an
29
30 320 image analysis system (Komet 6, Kinetic Imaging Ltd). At least 50 nuclei were analysed per slide, and
31
32 321 the percentage of DNA present in the comet tail (% tail DNA) was measured for each observed nucleus.

32 322

33
34 323 **2.6.2 Biliary PAH metabolites**

35
36
37 324 The analytical procedure used to quantify PAH metabolites (OH-naphthalenes, OH-phenanthrenes,
38
39 325 OH-pyrene, OH-benzo(a)pyrene) was adapted from Mazéas and Budzinski (2005) and Wessel et al.
40
41 326 (2013) . Bile samples (10-50 μL) are homogenised with 2 mL of acetate buffer pH5. After adding an
42
43 327 internal calibration solution (1-OH-Pyrene-d9 and 4-OH-Biphenyl-d9), an enzymatic deconjugation
44
45 328 step is performed at 37°C for 18 hours (β -glucuronidase from *Helix pomatia* type HP2 and 2-
46
47 329 mercaptoethanol). After deconjugation, the bile samples are extracted by solid phase extraction (SPE,
48
49 330 C18 cartridge 500 mg 3 mL). The organic extracts were eluted with 2 x 2 mL of methanol, concentrated
50
51 331 under gas flow at 50 μL and then re-dissolved in 1 mL of 80/20, v/v dichloromethane/methanol
52
53 332 mixture. The resulting extract were purified by solid phase extraction (SPE, NH2 cartridge, 500 mg, 3
54
55 333 mL), eluted with 2 x 2.5 mL of an 80/20, v/v dichloromethane/methanol mixture and concentrated
56
57 334 under gas flow at 100 μL in methanol. Finally, the extracts were stored at -20°C until injection. Mono-
58
59 335 hydroxylated PAH metabolites were analyzed by LC/MSMS in negative ionization mode (Infinity 1290
60
61 336 LC/6460 Triple Quad LC/MS, Agilent Technologies). The column used for analysis was an Acquity UPLC
62
63 337 BEH C18 (1.7 μm x 2.1 mm x 50 mm, Waters), the temperature of the column was set at 45°C . The

338 injected volume of organic extract was fixed at 5 μ L. The gradient of elution solvents was: ultra-pure
339 water/methanol (70/30) to methanol (100%) at 0.6 ml/min (6.5 min). Metabolites were quantified by
340 isotopic dilution in MRM mode. Various quality controls were carried out to validate the analytical
341 procedure. Protocol blanks were carried out in order to verify the absence of cross-contamination
342 during the laboratory sample processing process. The quantification limits and yields were carried out
343 by using spiked model matrix. Quantification limits were characterized and ranged from 1 to 3 ng g⁻¹
344 of bile depending the compounds. Recoveries ranged from 75 to 105% with mean variability of 20%.

345 **2.6.3 Tissue content in trace metal elements**

346 For both metal and organic contaminant analyses, tissues were freeze-dried and ground into a fine
347 powder. All contaminant concentrations are given in dry weight (dw).

348 In fish muscle, total mercury (Hg) concentrations were assessed by atomic absorption
349 spectrophotometry on aliquots of homogenised powder ($\sim 40 \pm 10$ mg), using an Advanced Mercury
350 Analyser (ALTEC AMA-254, Altec Ltd) and according to the standard operating procedure described in
351 the US-EPA method N°7473 (U.S. Environmental Protection Agency, 1998). With this method, the limit
352 of quantification (LOQ) for Hg determination in muscle was 0.015 mg kg⁻¹ dw.

353 In fish liver, total silver (Ag), arsenic (As), cadmium (Cd), cobalt (Co), copper (Cu), iron (Fe), mercury
354 (Hg), manganese (Mn), molybdenum (Mo), lead (Pb) and zinc (Zn) concentrations were determined
355 with a Quadrupole Inductively-Coupled Plasma Mass Spectrometer (Q-ICP-MS, ICAP-Qc model from
356 ThermoFisher), according to an in-laboratory approved method. Briefly, with this method, aliquots of
357 samples (~ 200 mg of homogenised powder) are placed in Teflon bombs and mineralised with a mixture
358 of ultrapure HNO₃ acid and milli-Q water, using a microwave (ETHOS-UP model from Milestone). The
359 digests are then diluted to 50 mL with milli-Q water before analyses with Q-ICP-MS. With this method,
360 LOQs (in mg kg⁻¹ dw) were 0.07 for Ag, Cd, Mo and Pb, 0.86 for As, 0.01 for Co, 0.93 for Cu, 8.6 for Fe,
361 0.06 for Hg, 0.69 for Mn and 9.3 for Zn.

362 The quality assurance of all metal analyses relied on blank and internal standard controls and on the
363 accuracy and reproducibility of data relative to the certified reference materials (CRMs) used in
364 analytical runs. The CRMs used were IAEA-407 (whole-fish homogenate; International Atomic Energy
365 Agency/IAEA) and IAEA-142 (mussel homogenate; IAEA) for Hg, as well as DORM-4 (fish protein,
366 National Research Council Canada/NRCC), DOLT-5 (dogfish liver, NRCC) and CE-278k (mussel tissue,
367 Joint Research Centre- European Commission) for the other trace metal elements. Blank values were
368 systematically below the detection limits, and CRM values concurred with certified concentrations,
369 with recovery rates ranging between 88 and 114% for all elements and CRMs.

370

371 **2.6.4 Organic contaminant analysis in fish muscle**

372 Detailed analytical procedures and QA/QC parameters for PCBs, OCPs, PBDEs and PFASs can be found
373 in Munsch et al. (2020b) and references therein. Method precision calculated as the relative standard
374 deviation of replicates was 2-17% for PCBs, 6-28% for OCP, 4-20% for PBDEs and 12-33% for PFASs

375 For PCBs (i.e. the 7 ICES priority congeners, namely CB-28, -52, -101, -118, -138, -153, -180), OCPs (five
376 dichlorodiphenyltrichloroethane (DDT) isomers, four hexachlorocyclohexane (HCH) isomers and
377 dieldrin) and PBDEs (8 congeners, namely BDE-28, -47, -49, -99, -100, -153, -154, -183), 5 g of freeze-
378 dried sample were extracted by pressurised liquid extraction with dichloromethane. Prior to
379 extraction, ¹³C₁₂-labelled compounds were added to the sample for internal standard calibration and
380 quantification using the isotopic dilution method. The extracts were successively purified using gel
381 permeation chromatography, a silica and alumina adsorption chromatography column and a two-
382 dimensional HPLC system with two columns coupled in series. Analyses were performed by gas
383 chromatography coupled to a high-resolution mass spectrometry (GC-HRMS), using a Hewlett-Packard
384 6890 gas chromatograph coupled to an AutoSpec Ultima mass spectrometer (Waters Corp.).

385 For PFASs, 1 gram of a freeze-dried sample, to which an internal standard mixture of nine labelled
386 compounds was added prior to agitation, was extracted using liquid-solid extraction with MeOH/KOH
387 (0.01 M of KOH), purified onto two consecutive SPE cartridges (a weak anion exchange (WAX)
388 stationary phase and a graphite (Envicarb) stationary phase), evaporated to dryness and reconstituted
389 in 200 µL of a mixture of MeOH/H₂O (50/50, v/v), containing the injection standard, PFOS ¹³C₈. Targeted
390 analytes (including C₄- to C₁₀-perfluoroalkyl sulfonates (PFASs) and C₆- to C₁₄ perfluorocarboxylic acids
391 (PFCAs)) were quantified using the corresponding isotope-labelled standard. Analysis was performed
392 using an Acquity ultra-performance liquid chromatograph (UPLC®, Waters Corp.) coupled to a triple
393 quadrupole mass spectrometer (Xevo® TQ-S micro, Waters Corp.) interfaced with a Z-spray™ (Waters
394 Corp.) electrospray ionisation source.

395

396 **2.10 Statistical analysis**

397 Means were always given with their respective standard error. Regression analysis were performed
398 using the software package Statistica 8.0 (General regression models, Pearson correlation coefficient).
399 The effect of sex on both TLs and DNA damage (4 males and 4 females) was studied by applying
400 nonparametric Mann-Whitney U tests (Statistica Soft. 8.0). Significant differences were considered at
401 $p < 0.05$.

402

403 3. Results

404 3.1 Age and sex distribution of flounders caught at ES station

405 The age and sex of the flounders caught during the survey at ES location are given in Figure 3. First, it
406 is noteworthy that for the same length class, age could vary from 1 to 3 years. Otolith analysis showed
407 that 60% of the flounders sampled were 2 years old (67 and 50% males and females, respectively).

408 3.2. Validation of the QPCR assay for the measurement of TL in the flounder

409 Regarding the MIQE Guidelines, the PCR efficiencies of the different sets of primers used for the
410 amplification of the telomeric sequence and the single-copy gene using either composite DNA or
411 standard oligomers were all validated, with values between 98 and 104% (Table 2). This is illustrated
412 in Figure 4 for the amplification of the telomeric sequence and the GAPDH gene in the composite DNA
413 sample. For the telomere and GAPDH oligomers, standard curves were obtained to allow absolute TL
414 measurement (Figure 5).

415 TL data are presented only for 2-year-old flounders (see 3.3) as the number of fish from the other age
416 classes was insufficient.

417 3.3 TLs and level of DNA damage in 2-year-old flounders from the Seine Bay

418 The relative and absolute TLs were 0.811 ± 0.017 and 54.3 ± 12.8 kbp, respectively (mean \pm standard
419 error). Considering the number of chromosomes in the flounder ($2N = 48$, Saygun, 2015), the mean
420 length of a telomere unit is around 0.57 ± 0.13 kb (mean \pm standard error). Relative and absolute TLs
421 were negatively correlated ($R^2 = 0.925$, $p < 0.001$) (Figure 6). The longer is the TL and the lower are the
422 corresponding Ct value and T/S ratio. Irrespective of relative or absolute TL, no difference was
423 observed between female and male flounders (Mann Whitney U tests, $n = 4$ per sex, $p = 0.69$ and $p =$
424 0.34 , respectively).

425 In the erythrocytes, application of the comet assay gave a % tail DNA value of 15.71 ± 3.72 (mean \pm
426 standard error), with no difference between fish sex ($n = 4$ per sex, $p = 0.99$).

427 3.4 Chemical contamination of 2-year-old flounders

428 3.4.1 Tissue concentrations of trace metal elements (TMEs)

429 The measured concentrations for TMEs in the liver (Ag, As, Cd, Co, Cu, Fe, Hg, Mn, Mo, Pb, Zn) and in
430 the muscle (Hg) are reported in Table 3.

431

432 3.4.2 Levels of biliary PAH metabolites

433 One- and 2-hydroxy metabolites of naphthalene were detected above the quantification limit in only
434 two individuals (concentrations of 6 ng g⁻¹ bile). In contrast, hydroxyl metabolites of phenanthrene
435 were detected in nearly all fish analysed, with the exception of one individual; most of these
436 metabolites (76%) were made of 2-OH and 3-OH. Nine-OH BaP was the only detected BaP metabolite
437 in fish bile, with the exception of one individual (26 ± 10 ng g⁻¹). The major PAH metabolite was 1-OH
438 pyrene (226 ± 78 ng g⁻¹ bile), representing more than 80% of the total measured PAH metabolites in
439 fish bile (Σhydroxylated PAH metabolites of 260 ± 90 ng g⁻¹ bile).

440 3.4.3 Levels of PCBs, OCPs, PBDEs and PFASs in flounder muscle

441 In all samples, PCB and PBDE congeners, DDT isomers, dieldrin, PFOS and long-chain PFASs were above
442 the LOQs, while among HCH isomers, δ-HCH was below the LOQ in three out of eight analysed fish.
443 The highest concentrations were found for PCBs (97.2 ± 25.3 ng g⁻¹ dw), followed by PFASs (4.85 ± 1.48
444 ng g⁻¹ dw), OCPs (2.57 ± 0.66 ng g⁻¹ dw) and PBDEs (0.51 ± 0.14 ng g⁻¹ dw) (Table 4). Highly significant
445 correlations were found between PCB, OCP, PBDE and PFAS concentrations (R² between 0.61 and 0.98,
446 p < 0.05).

447 Although the significance of sex-related differences in POP concentrations could not be tested because
448 of a limited number of samples of each sex, no tendency in POP concentrations was observed between
449 male and female individuals. The results were therefore considered for both sexes together.

450 **3.4 Correlations between TLs, DNA damage and chemical contamination in flounders**

451 Regardless of considering relative or absolute TL, no correlation was observed with the percentage of
452 tail DNA and any of the chemical contaminants measured in flounder tissue when considering
453 statistical significance from a p-value < 0.05 (Table 5). However, relative TL could be positively
454 correlated to OCPs, DDT and PCBs by increasing the α risk value from 0.05 to 0.10 (e. g. the p-value
455 associated to the coefficient of determination between relative TL and DDT is 0.05 < 0.081 < 0.10). In
456 this study, the percentage of tail DNA was not correlated with chemical contamination (Table 5).
457 Considering individual trace elements rather than their sum did not change the results, except for Mn
458 and Fe, which were positively correlated to the % tail DNA (p = 0.021 and p = 0.007, respectively).

459 **4. Discussion**

460 **4.1 Telomere length is species-specific, and its value can vary depending on the methods used for** 461 **its measurement**

463 In the present study, a first measurement of TL by q-PCR was realised in the flounder (mean absolute
1 464 TL of 54.3 kpb/diploid genome, mean of a telomere unit length of 0.57 kpb). It was possible to compare
2 465 this result to other published data obtained in fish species using either TRF or the Telomere Amount
3 466 and Length Assay (TALA) technique. Telomere length varies between fish species when comparing data
4 467 obtained in the European sea bass *Dicentrarchus labrax* (2.8-4.9 kb, TRF technique, Horn et al., 2008),
5 468 the killifish *Fundulus heteroclitus* (2.0–10.0 kb, TALA technique, Elmore et al., 2008), the American eel
6 469 *Anguilla rostrata* (10.0–15.0 kb, TALA technique, Elmore et al., 2008), the rainbow trout *Oncorhynchus*
7 470 *mykiss* (up to 20 kb, TRF technique, Leijnin et al., 1995), the Japanese medaka *Oryzias latipes* (3.0–12.0
8 471 kb, TALA technique, Elmore et al., 2008) and the zebrafish *Dana rerio* (2.0–10.0 kb, TALA technique,
9 472 Elmore et al., 2008). However, comparisons must be done with care, as in recent years, several papers
10 473 dealt with the different techniques used to measure TL and their respective limitations. Among all the
11 474 techniques developed, the TRF is often described as the “gold standard” method, despite its
12 475 disadvantages (Montpetit et al., 2014, Wang et al., 2018); it requires high amounts of DNA and is
13 476 labour-intensive and costly. The restriction enzymes used result in the inclusion of subtelomeric DNA,
14 477 which is contiguous to the telomere, thereby leading to a possible overestimation of TL. It is also unable
15 478 to detect short telomeres due to limited binding of the probe used for detection. In contrast, q-PCR-
16 479 based techniques are well suited for high-throughput analyses due to their simplicity and low costs.
17 480 The q-PCR-based techniques have, however, a primer dimerisation problem, which can be overcome
18 481 by choosing primers that bind to the C- and G-rich segments but are mismatched at the other bases
19 482 and by decreasing the temperature of the first cycles (Cawthon, 2009). However, the results from these
20 483 studies are limited in their ability to allow for comparisons between studies due to relatively high levels
21 484 of variation (Wang et al., 2018). The DNA extraction method, the storage conditions of the DNA,
22 485 telomere primer sequences, master mixes made by different vendors or homemade master mixes are
23 486 some examples of factors potentially impacting the assay (Martin-Ruiz et al., 2015, Lin et al., 2019).
24 487 Moreover, the use of conversion equations to determine TL in kb is the source of a higher degree of
25 488 bias in the TL values calculated by q-PCR techniques. Other attributes also warrant consideration, such
26 489 as the biological specimen to be evaluated. In the case of blood, which was analysed in the present
27 490 study, results reflect the lengths of the various blood cells that divide at different rates. Whereas
28 491 granulocytes (including neutrophils, eosinophils and basophils) have a lifespan of hours to days,
29 492 agranulocytes (including lymphocytes and monocytes) can have a lifespan of days to years (Montpetit
30 493 et al., 2014). Moreover, a different ratio of cell types could add variability and explain some of the
31 494 variations previously reported among different tissues (Lin et al., 2019, Morinha et al., 2020). As
32 495 concluded by a recent published international inter-calibration exercise (Martin-Ruiz et al., 2015),
33 496 there is a need for protocol homogenisation to allow comparisons of TL data obtained by different
34 497 laboratories in various published studies (Lai et al., 2018, Lin et al., 2019).

498 TL data obtained by q-PCR are still scarce in aquatic species. Izzo et al. (2010) reported TL values per
1 499 diploid genome between 86 and 590 kb in the muscle of the shark *Heterodontus portusjacksoni*, 12
2
3 500 and 585 kb in the muscle of carp *Cyprinus carpio* and 16 and 388 kb in the hind flipper biopsy of the
4
5 501 sea lion *Neophoca cinerea*, depending on the age.
6

7 502

8 503 **4.2 Considering the influence of fish ontogenetic stage and sex on biomarker responses is of** 9 10 504 **paramount importance**

11
12
13 505 In the present study, it was initially decided to work only on fish from the same age and sex to take
14
15 506 into account the influences of these biotic factors on the measured chemical and biological markers.
16
17 507 Because age and sex could only be *a posteriori* established by otolith analysis and gonad examination,
18 508 respectively, the control over the sampling program was not total during the survey and the sampling
19
20 509 effort was significantly reduced afterward when constituting a subsample of fish from the same
21
22 510 ontogenetic stage and sex.
23

24 511 In flatfish, the response of classical biomarkers used in ecotoxicology and for biomonitoring purposes
25
26 512 varies with body length (used as a proxy of age) and sex. In dab from the Seine Estuary, DNA strand
27
28 513 breaks and 7-ethoxyresorufin-O-deethylase activity are influenced by both factors (Akcha et al., 2004,
29
30 514 Devier et al., 2013). Similar observations have been reported for the European flounder from the Baltic
31
32 515 Sea, concerning the response of other enzymatic biomarkers, namely the acetylcholinesterase and the
33 516 glutathione S-transferase activities (Napierska et al. 2005). These effects are likely related to the
34
35 517 existence in fish of differences with sex and age in their ability to bioaccumulate and biotransform
36
37 518 contaminants. For example, metal bioaccumulation (mercury, copper and zinc) depends on age in
38 519 several coastal fish species including the flounder; a normalisation technique was even recently
39
40 520 proposed to take this confounding factor into account and to allow reliable inter-site comparisons
41
42 521 (Suhareva et al., 2020). This is also the case for organic contaminants such as PCBs, for which
43
44 522 differences with sex have also been observed in several species, with higher concentrations expected
45
46 523 in males due to a higher energy expenditure rate (high resting metabolic rate and greater swimming
47 524 activity) compared to females (Mandénjian et al., 2016, Mandénjian, 2020). As a consequence, the
48
49 525 JAMP Guidelines for Contaminant-specific Biological Effects Monitoring (OSPAR Agreement Ref. No.
50
51 526 2008-09) highly recommended to consider the influences of these biotic factors when designing
52
53 527 sampling programs; therefore, monitoring should be performed during a relatively stable physiological
54
55 528 status and, in any case, during a period before spawning.

56 529 Concerning TL, the choice to analyse fish from the same age was particularly important due to the
57
58 530 highly probable ontogenetic effect on TL. Telomeres play a crucial role in protecting the chromosomes
59
60 531 at each cell cycle. This effect has already been investigated in different roundfish species with different
61

532 findings. Telomere shortening with age is not verified for all species, probably due to active telomerase
1 533 activity and complex telomere dynamics in fish. In humans, telomerase expression in adults is
2 534 restricted to germ line cells, stem cells and tumours (Cong et al., 2002); it is expressed in all tissues
3 535 throughout the whole life of many fish species. This is also the case in the adult rainbow trout,
4 536 *Oncorhynchus mykiss*, for which high telomerase activities were measured in all analysed tissues using
5 537 the Telomerase Repeated Amplification Protocol (TRAP) assay, with the highest activities measured in
6 538 the liver and the kidney (Klapper et al., 1998). Telomerase activity was also demonstrated by RTQ (real-
7 539 time quantitative)-TRAP assay in the muscle of several species, such as the flounder (McChesney et al.,
8 540 2005) and model laboratory fish such as the marine medaka, *Oryzias melastigma* (Peterson et al., 2015)
9 541 and the zebrafish *Brachydanio rerio* (Anchelin et al., 2011). The way TL evolves with age appears to be
10 542 different depending on the species. In the Atlantic Salmon *Salmo salar*, TL increased between embryo
11 543 and larvae stage (McLennan et al., 2018) whereas it decreased between smolt and adult stages during
12 544 a longitudinal study based on a recapture experiment that allowed TL measurement in the same
13 545 individuals before and after migration (MacLennan et al., 2017). In the long-lived sturgeon *Acipenser*
14 546 *baerii*, telomere shortening with age was also observed (Simide et al., 2016) whereas in the European
15 547 seabass *Dicentrarchus labrax*, no correlation was observed between TL and age (Horn et al., 2008). It
16 548 is noteworthy that for some species, such as the zebrafish, the way telomere length evolves with age
17 549 seems to be directly dependent on the tissue type. By analysing the whole body, Anchelin et al. (2011)
18 550 showed a non-linear age-related variation in TL, with an increase from larvae to adult stage and a
19 551 significant telomere shortening in aged fish. By analysing different zebrafish tissues, Carneiro et al.
20 552 (2016) showed that telomeres shorten to critical lengths with age only in specific tissues (e.g. gut,
21 553 muscle), independently of their proliferation rate. To our knowledge, variation of TL with age has not
22 554 yet been investigated in flatfish. There is, however, a strong interest in determining telomere
23 555 shortening rates in these widely used sentinel species, as these data correlate to the lifespan in many
24 556 birds and mammals (Whittemore et al., 2019).

25 557 In the present paper, no difference in TL was observed with sex. However, the number of samples was
26 558 limited, requiring further confirmation. Different findings were reported in the bibliography
27 559 concerning the influence of sex on TL in fish. In the common carp *Cyprinus carpio*, Izzo et al. (2014)
28 560 showed no difference with sex or states of sexual maturity in muscle and fin clip telomere lengths. In
29 561 contrast, sex differences in longevity and telomere length were observed in the marine medaka, both
30 562 being higher in females than in males (Yip et al., 2017). In the females, the level of plasma E2 was
31 563 shown to be positively correlated with TL. These results were consistent with the previous
32 564 demonstration, in this species, of sex difference in telomerase activity (female > male) upon sexual
33 565 maturation (Peterson et al., 2015).

566

1 567
2

3 568 **4.3 Telomere length can vary under the influence of environmental factors such as chemical**
4
5 569 **pollution**

6
7 570 Telomere length is also under the influence of environmental factors such as chemical contamination,
8
9 571 which can modify telomere dynamics and, as a consequence, the rate of telomere loss in fish. The
10
11 572 chemical analyses performed in the present study showed that flounders from the Seine Estuary are
12
13 573 exposed to mixtures of chemical contaminants, as previously reported in dab with the detection of
14
15 574 PCBs, dioxins, furanes and PAHs in fish tissue and bile, respectively (Munsch et al., 2004, Devier et al.,
16
17 575 2012), and in various vertebrate and invertebrate species for several historic and emerging
18
19 576 contaminants (Tappin and Millward, 2015).

20 577 Exposure to these complex contaminant mixtures is responsible for a genotoxic stress in dab from the
21
22 578 Seine Estuary (Akcha et al., 2003, 2004, Munsch et al., 2004, Devier et al., 2012). This could also be
23
24 579 the case in flounders, presenting a similar level of DNA strand breaks. In fact, PAHs (Le Du-Lacoste et
25
26 580 al., 2012), PCBs (Marabini et al., 2011), PBDEs (Sharma et al., 2018), OCPs and PFASs (Ayanda et al.,
27
28 581 2018) are genotoxic in fish, which explains why in several fish species, correlations were previously
29
30 582 observed between chemical body burden and level of DNA strand breaks. This is the case in dab from
31
32 583 the Seine Estuary, for which correlations were observed with PAH metabolites, PCBs (Σ PCBs and
33
34 584 Σ 7PCBs: CB-28, -52, -101, -118, -138, -153, -180) and PCDDs/PCDFs (Akcha et al., 2005, Devier et al.,
35
36 585 2012). Correlations were also observed in the European flounder from the Baltic Sea when using lipid-
37
38 586 based concentrations of PCB 118, Σ 7PCB and Σ m-oPCB (mono-ortho chlorinated congeners: CB-114, -
39
40 587 118, -105, -156, -157, -167, -189) (Dabrovska et al., 2014) and in the Californian halibut *Paralichthys*
41
42 588 *californicus* from Southern California bays and harbours with PAH metabolites (Brown and Steinert,
43
44 589 2003). In the present study, no correlation between chemical contamination and the level of % tail
45
46 590 DNA was observed in flounders. The same observation was made for TL, which did not appear to be
47
48 591 correlated with any of the contaminants measured in our study. Because we analysed a limited number
49
50 592 of fish, all coming from the same area, this point requires further investigations, motivated by the
51
52 593 positive correlations between relative TL and organochlorinated compounds (PCBs, DDT and OCPs),
53
54 594 which could be observed when increasing the α risk value from 0.05 to 0.10. Telomeres are particularly
55
56 595 sensitive to oxidative damage (Monaghan et al., 2018), which is induced by a wide range of
57
58 596 environmental contaminants such as those measured in the present study (Valavanidis et al., 2006,
59
60 597 Lushchak 2015). One reason for increased vulnerability is the presence of a high proportion of guanine
61
62 598 bases in the telomeric sequence, which target oxyradicals (Honda et al., 2001, Kawanishi and Oikawa
63
64 599 2004). The underlying mechanisms of telomere loss by oxidative DNA lesions have been investigated
65

600 by several authors, who pointed out a replication fork collapse in the telomere region (e.g. Coluzzi et
1 601 al., 2019).

3 602 The impact of chemical pollution on telomeres was mainly investigated in humans, with a high number
4 603 of epidemiology and toxicology studies in the last decades. Based on the results, TL can be affected in
5 604 different ways (decrease, increase or no effect), depending on e.g. the chemical contaminants studied,
6 605 the mode of exposure and the type of cells analysed (Louzon et al., 2019, Ng and Amini, 2020). For
7 606 example, exposure to PCBs and OCPs (as measured by their serum levels) was shown to impact
8 607 leukocyte TL in humans (Karimi et al., 2020), whereas non-dioxin-like PCBs and dioxin-like PCBs (except
9 608 for CB28) were related to increased TL; OCP exposure was related to telomere shortening. In another
10 609 study focusing on children exposed to traffic-related air pollution, an inverse linear relationship was
11 610 demonstrated between PAH level (daily individual exposure) and TL in peripheral blood mononuclear
12 611 cells (Lee et al., 2017). Effects were also reported for PFASs for which prenatal exposure was associated
13 612 with a significant decrease in leukocyte TL, but only in female new-borns (Liu et al., 2018). By using *in*
14 613 *vitro* approaches, many contaminants were shown to interact with telomerase-related gene
15 614 expression, telomerase activity and telomere shelterins, modifying telomere dynamics (Xin et al., 2016,
16 615 Kahl et al., 2016, Ling et al., 2018). The same appears to be true for animals, particularly for birds, albeit
17 616 with a more limited number of studies. In adult female black-legged kittiwakes *Rissa tridactyla*, a
18 617 negative correlation was found between blood concentration of oxychlordan (major metabolites of
19 618 chlordan-related contaminants) and TL (Blevin et al., 2016). The impact of PFASs was also investigated
20 619 in this species, with different findings. In adults, no association could be determined between exposure
21 620 to PFASs and absolute TL, with the exception of significantly elongated telomeres in birds presenting
22 621 the highest concentration of PFASs (Blévin et al., 2017). In chicks of white-tailed eagles *Haliaeetus*
23 622 *albicilla*, no relationship between the concentrations of organohalogenated compounds (PCBs, DDT,
24 623 HCH, HCB: hexachlorobenzene) and TL was observed, despite significant changes in the antioxidant
25 624 enzyme superoxide dismutase, plasma non-enzymatic antioxidant capacity and oxidative damage to
26 625 plasma proteins (Sletten et al., 2016, Costantini et al., 2019). In contrast, in the adult glaucous gull
27 626 *Larus hyperboreus*, some single PFAS compounds are positively correlated with the slowest rate of
28 627 telomere shortening (Sebastiano et al., 2020). Similar to humans, the, contaminant effect on telomere
29 628 dynamics in birds seems to vary according to the nature of the contaminant and the species. In flatfish,
30 629 more investigations are needed to conclude on this point.

31 630 Similar to DNA strand breaks, telomere shortening in flounders could occur following oxyradical
32 631 production related to contaminant exposure. As mentioned previously, DNA damage can contribute
33 632 directly to telomere attrition due to replication fork collapse. Therefore, the absence of a relationship
34 633 between these two types of genome damage can appear inconsistent. There could be, however, a bias

634 in the direct comparison of both markers, as changes in TL could be more integrative of a cumulative
635 damage produced by oxyradical attacks due to a more reduced repairing capacity than for DNA strand
636 breaks.

637 **5. Conclusion**

638 A protocol for TL measurement was adapted with success in the European flounder, widely used as
639 sentinel species in biomonitoring studies. It was then applied to a limited number of samples caught
640 in the Seine Estuary. In the absence of knowledge on the relationship between TL and age in this
641 species, fish age was determined in the laboratory by otolith sclerochronology to analyse only fish from
642 the same age, thereby limiting ontogenic variability among specimens. This requirement significantly
643 reduced the sampling effort, highlighting the necessity to increase fish catching in the field for this kind
644 of investigations, raising ethical and economic issues.

645 Because exposure to chemical contaminants could affect TL in flounder, we looked for correlations
646 with chemical body burden, which were not found. Due to the limited number of fish analysed and the
647 lack of knowledge on telomere dynamics in flatfish (e.g. age and sex effect, tissue effect, level of
648 telomerase activity), it is necessary to perform further investigations, motivated by the correlations
649 that were observed with organochlorinated compounds when decreasing statistical significance (α
650 value from 0.05 to 0.10). In addition to field studies based on several contrasted sites, it will be
651 particularly interesting to conduct controlled experiments at the laboratory for individual widely
652 distributed environmental contaminants and mixtures thereof. Determining the telomere shortening
653 rate following chemical stress could hence provide evidence of an impact of chemical pollution on the
654 lifespan of flatfish populations, as demonstrated for human and several animal species. Because
655 flatfish species can present differences in sensitivity to chemical pollutants, work should also be
656 conducted in more vulnerable species (e.g. *Solea solea*).

657 **Acknowledgement**

659 This work was supported by the French Research Institute for Sea Exploration (Ifremer) and the Water
660 Agency of the Seine-Normandie. We are grateful to the technical and scientific crews of R/Vs Antea for
661 their work during the sea survey. Nadège Bely, Nathalie Olivier, Sylvette Crochet, Sandrine Bruzac,
662 Charles Pollono, Teddy Sireau, Thomas Bastien, Karyn Le Menach and Patrick Pardon are gratefully
663 acknowledged for performing organic and inorganic contaminant analyses and assuring QA/QC;
664 Romain Elleboode performed otolith analysis. The platform PLATINE is also acknowledged for technical
665 support in PAH metabolites analysis.

666

667 **References**

- 1
2 668
3 669 Akcha F., Hubert F., Pfohl-Leszkowicz A. (2003). Potential value of the comet assay and DNA adduct
4 measurement in dab (*Limanda limanda*) for assessment of *in situ* exposure to genotoxic compounds.
5 670 Mutat Res Gen Tox En 534: 21-32, DOI: 10.1016/S1383-5718(02)00244-9.
6
7 671
8
9 672
10 673 Akcha F., Leday G., Pfohl-Leszkowicz A. (2004). Measurement of DNA adducts and strand breaks in dab
11 (*Limanda limanda*) collected in the field: effects of biotic (age, sex) and abiotic (sampling site and
12 674 period) factors on the extent of DNA damage. Mutat Res Fund Mol M 552: 197-207, DOI:
13 675 10.1016/j.mrfmmm.2004.06.020.
14
15 676
16
17 677
18
19 678 Akcha F., Munsch C., Moisan K., Tronczynski J. (2005). Relation entre la contamination chimique de
20 l'Estuaire de la Seine et les effets génotoxiques et cancérigènes chez la limande. Ifremer,
21 679 R.INT.DCN/BE- 2005-08, pp 70.
22
23 680
24
25 681
26 682 Andrei R. C., Cristea V., Crețu M., Dediu L., Mogodan A. (2018). The effect of temperature on the
27 standard and routine metabolic rates of young of the year sterlet sturgeon (*Acipenser ruthenus*). AACL
28 683 Bioflux, 11: 1467-1475.
29
30 684
31
32 685
33 686 Auer S. K., Salin K., Anderson G. J., Metcalfe N. B. (2018). Individuals exhibit consistent differences in
34 their metabolic rates across changing thermal conditions. Comp Biochem Physiol A Mol Integr Physiol
35 687 217: 1–6, DOI: 10.1016/j.cbpa.2017.11.021.
36
37 688
38
39 689
40 690 Ayanda I. O., Yang M., Y. Zhang, Zha J. (2018). Cytotoxic and genotoxic effects of perfluorododecanoic
41 acid (PFDoA) in Japanese medaka. Knowl Manag Aquat Ecosyst 419: 9, DOI: 10.1051/kmae/2017058.
42 691
43
44 692
45 693 Axson E. L., Peterson K. E., Tellez-Rojo M. M., Goodrich J. M., Meeker J., Mercado-García A., Solano M.,
46 Needham B. L. (2018). Sex differences in telomere length are not mediated by sex steroid hormones
47 or body size in early adolescence. Gend Genome 2: 68-75, DOI: 10.1177/2470289718795177.
48 694
49 695
50
51 696
52 697 Barnes R. P., Fouquerel E., Opresko P. L. (2019). The impact of oxidative DNA damage and stress on
53 telomere homeostasis. Mech Ageing Dev 177: 37-45, DOI: 10.1016/j.mad.2018.03.013.
54 698
55
56 699
57
58 700 Barranger A., Akcha F., Rouxel J., Brizard R., Maurouard E., Pallud M., Menard D., Tapie N., Budzinski
59 H., Burgeot T., Benabdelmouna A. (2014). Study of genetic damage in the Japanese oyster induced by
60 701
61
62
63
64
65

702 an environmentally-relevant exposure to diuron: evidence of vertical transmission of DNA damage.
1
2 703 *Aquat Toxicol* 146: 93-104, DOI: 10.1016/j.aquatox.2013.10.032.
3
4 704
5 705 Blévin P., Angelier F., Tartu S., Ruault S., Bustamante P. (2016). Exposure to oxychlorodane is associated
6
7 706 with shorter telomeres in arctic breeding kittiwakes. *Sci Total Environ* 563-564: 125-130, DOI:
8
9 707 10.1016/j.scitotenv.2016.04.096.
10
11 708
12 709 Blévin P., Angelier F., Tartu S., Bustamante P., Herzke D., Moe B., Chastel O. (2017). Perfluorinated
13
14 710 substances and telomeres in an Arctic seabird: Cross-sectional and longitudinal approaches. *Environ*
15
16 711 *Pollut* 230: 360-367, DOI: 10.1016/j.envpol.2017.06.060.
17
18 712
19 713 Brown J. S. and Steinert S. A. (2003). DNA damage and biliary PAH metabolites in flatfish from Southern
20
21 714 California bays and harbors, and the Channel Islands. *Ecol Indic* 3: 263–274, DOI:
22
23 715 10.1016/j.ecolind.2003.11.004.
24
25 716
26 717 Bustin S. A., Benes V., Garson J. A., Hellemans J., Huggett J., Kubista M., Mueller R., Nolan T., Pfaffl M.
27
28 718 W., Shipley G. L., Vandesompele J., Wittwer C. T. (2009). The MIQE Guidelines: Minimum Information
29
30 719 for Publication of Quantitative Real-Time PCR Experiments. *Clin Chem*, 55: 611–622, DOI:
31
32 720 10.1373/clinchem.2008.112797.
33
34 721
35 722 Carneiro M. C., Henriques C. M., Nabais J., Ferreira T., Carvalho T., Ferreira M. G. (2016). Short
36
37 723 telomeres in key tissues initiate local and systemic aging in zebrafish. *PLoS Genet* 12: e1005798, DOI:
38
39 724 10.1371/journal.pgen.1005798.
40
41 725
42 726 Cawthon R. M. (2009). Telomere length measurement by a novel monochrome multiplex quantitative
43
44 727 PCR method. *Nucleic Acids Res* 37: e21, DOI: 10.1093/nar/gkn1027.
45
46 728
47 729 Coluzzi E., Leone S., Sgura A. (2019). Oxidative stress induces telomere dysfunction and senescence by
48
49 730 replication fork arrest. *Cells* 8: 19, DOI: 10.3390/cells8010019.
50
51 731
52
53 732 Cong Y-S., Wright W. E., Shay J. W. (2002). Human telomerase and its regulation. *Microbiol Mol Biol R*
54
55 733 *66*: 407-425, DOI: 10.1128/MMBR.66.3.407–425.2002.
56
57 734
58
59
60
61
62
63
64
65

735 Dabrowska H., Kopko O., Góra A., Waszak I., Walkusz-Miotk J. (2014). DNA damage, EROD activity,
1 736 condition indices, and their linkages with contaminants in female flounder (*Platichthys flesus*) from the
2 southern Baltic Sea. *Sci Total Env* 496 : 488-498, DOI:10.1016/j.scitotenv.2014.07.079.
3 737
4 738
5 739
6 740 Devier M-H., Le Du-Lacoste M., Akcha F., Morin B., Peluhet L., Le Menach K., Burgeot T., Budzinski H.
7 (2013). Biliary PAH metabolites, EROD activity and DNA damage in dab (*Limanda limanda*) from Seine
8 Estuary (France). *Environ Sci Pollut Res* 20: 708-722, DOI: 10.1007/s11356-012-1345-7.
9 741
10 742
11 743 Diopere E., Maes G. E., Komen H., Volckaert F. A. M., Groenen M. A. M. (2014). A genetic linkage map
12 of Sole (*Solea solea*): A tool for evolutionary and comparative analyses of exploited (flat)fishes. *PLoS*
13 *One*, 9: e115040, DOI: 10.1371/journal.pone.0115040.
14 744
15 745
16 746
17 747 Drevs T., Kadakas V., Lang T., Mellergaard S. (1999). Geographical variation in the age/length
18 relationship in Baltic flounder (*Platichthys flesus*). *ICES J Mar Sci*, 56: 134–137, DOI:
19 10.1006/jmsc.1999.0460.
20 748
21 749
22 750
23 751 Elmore L. W., Norris M. W., Sircar S., Bright A. T., McChesney P. A., Winn R. N., Holt S. E. (2008).
24 Upregulation of telomerase function during tissue regeneration. *Exp Biol Med* 233:958-67, DOI:
25 10.3181/0712-RM-345.
26 752
27 753
28 754
29 755 Flipo N., Lestel L., Labadie P., Meybeck M., Garnier J. (2020) Trajectories of the Seine River Basin. In:
30 The Handbook of Environmental Chemistry. Springer, Berlin, Heidelberg.
31 https://doi.org/10.1007/698_2019_437.
32 756
33 757
34 758
35 759 Foote C.G., Vleck D., Vleck C. M. (2013). Extent and variability of interstitial telomeric sequences and
36 their effects on estimates of telomere length. *Mol Ecol Res* 13: 417–428, DOI: 10.1111/1755-
37 0998.12079.
38 760
39 761
40 762
41 763 Gardner M., Bann D., Wiley L., Cooper R., Hardy R., Nitsch D., Martin-Ruiz C., Shiels P., Sayer A. A.,
42 Barbieri M., Bekaerth S., Bischoff C., Brooks-Wilson A. et al. (2014). Gender and telomere length:
43 Systematic review and meta-analysis. *Exp Gerontol* 51: 15-27, DOI: 10.1016/j.exger.2013.12.004
44 764
45 765
46 766
47 767 Harley C. B., Futcher A. B., Greider C. W. (1990). Telomeres shorten during ageing of human fibroblasts.
48 *Nature* 345: 458-460, DOI: 10.1038/345458a0.
49 768
50 769
51
52
53
54
55
56
57
58
59
60
61
62
63
64
65

770 Horn T., Gemmell N. J., Robertson B. C., Bridges C. R. (2008). Telomere length change in European sea
1 771 bass (*Dicentrarchus labrax*). Aust J Zool 56: 207–210, DOI: 10.1071/ZO08046.
2
3 772
4
5 773 Izzo C. (2010). Patterns of telomere length change with age in aquatic vertebrates and the phylogenetic
6 774 distribution of the pattern among jawed vertebrates. Thesis University of Adelaid School of Earth and
7 775 Environmental Science, <http://hdl.handle.net/2440/63477>.
8
9 776
10
11 777 Izzo C, Bertozzi T., Gillanders B., Donnellan S. (2014). Variation in telomere length of the common carp,
12 778 *Cyprinus carpio* (Cyprinidae), in relation to body length. Copeia 1: 87-94, DOI: 10.1643/CI-11-162.
13
14 779
15
16 780 Karimi B., Nodehib R. M., Yunesian M. (2020). Serum level of PCBs and OCPs and leukocyte telomere
17 781 length among adults in Tehran, Iran. Chemosphere 248: 126092, DOI:
18 782 10.1016/j.chemosphere.2020.126092
19
20
21 783
22
23 784 Kahl V. F. S., da Silva J., da Silvia F. R. (2016). Influence of exposure to pesticides on telomere length in
24 785 tobacco farmers: A biology system approach. Mutat Res Fund Mol 791-792: 19-26 DOI:
25 786 10.1016/j.mrfmmm.2016.08.003.
26
27
28 787
29
30 788 Lacaze E., Geffard O., Goyet D., Bony S., Devaux A. (2011). Linking genotoxic responses in *Gammarus*
31 789 *fossarum* germ cells with reproduction impairment, using the Comet assay. Environ Res 111: 626-634,
32 790 DOI: 10.1016/j.envres.2011.03.012.
33
34
35 791
36
37 792 Le Du-Lacoste M., Akcha F., Devier M-H., Morin B., Burgeot T., Budzinski H. (2013). Comparative study
38 793 of different exposure routes on the biotransformation and genotoxicity of PAHs in the flatfish species,
39 794 *Scophthalmus maximus*. Environ Sci Pollut Res 20: 690-707, DOI: 10.1007/s11356-012-1388-9.
40
41
42 795
43
44 796 Lee E. Y., Lin J., Noth E. M., Hammond S. K., Nadeau K. C., Eisen E. A., Balmes J. R. (2017). Traffic-related
45 797 air pollution and telomere length in children and adolescents living in Fresno, CA: A Pilot Study. J Occup
46 798 Environ Med 59: 446–452, DOI: 10.1097/JOM.0000000000000996.
47
48
49 799
50
51 800 Lei M., Zhang L., Lei J., Zong L., Li J., Wu Z., Wang Z. (2015). Overview of emerging contaminants and
52 801 associated human health effects. Biomed Res Int ID 404796, DOI: 10.1155/2015/404796.
53
54
55 802
56
57 803 Lejnine S., Makarov V. L., Langmore J. P. (1995). Conserved nucleoprotein structure at the ends of
58 804 vertebrate and invertebrate chromosomes. PNAS 92: 2393-2397, DOI: 10.1073/pnas.92.6.2393.
59
60
61
62
63
64
65

805

1
2 806 Ling X., Yang W., Zou P., Zhang G., Wang Z., Zhang X., Chen H., Peng K., Han F., Liu J., Cao J., Ao L.
3 807 (2018). TERT regulates telomere-related senescence and apoptosis through DNA damage response in
4
5 808 male germ cells exposed to BPDE *in vitro* and to B[a]P *in vivo*. Environ Pollut 235: 836-849, DOI:
6
7 809 10.1016/j.envpol.2017.12.099.

8
9 810
10 811 Liu H., Chen Q., Lei L., Zhou W., Huang L., Zhang J., Chen D. (2018). Prenatal exposure to perfluoroalkyl
11
12 812 and polyfluoroalkyl substances affects leukocyte telomere length in female newborns. Environ Pollut
13
14 813 235: 446-452, DOI: 10.1016/j.envpol.2017.12.095.

15
16 814
17 815 Louzon M., Coeurdassier M., Gimbert F., Pauget B., de Vaufleury A. (2019). Telomere dynamic in
18
19 816 humans and animals: Review and perspectives in environmental toxicology. Environ Int 131: 105025,
20
21 817 DOI: 10.1016/j.envint.2019.105025

22
23 818
24
25 819 Lushchak V. I. (2015). Contaminant-induced oxidative stress in fish: a mechanistic approach. Fish
26
27 820 Physiol Biochem 42: 711–747, DOI: 10.1007/s10695-015-0171-5.

28 821
29
30 822 Madenjian C. P., Rediske R. R., Krabbenhoft D. P., Stapanian M. A., Chernyak S. M., O'Keefe J. P. (2016).
31
32 823 Sex differences in contaminant concentrations of fish: A synthesis. Biol Sex Differ 7:42, DOI:
33
34 824 10.1186/s13293-016-0090-x.

35 825
36
37 826 Madenjian C. P. (2020). Males exceeding females in whole fish polychlorinated biphenyl concentration
38
39 827 mainly attributable to higher energy expenditure rate. Environ Toxicol Chem, 39: 951–952, DOI:
40
41 828 10.1002/etc.4685.

42 829
43
44 830 Marabini L., Calò R., Fucile S. (2011). Genotoxic effects of polychlorinated biphenyls (PCB 153, 138,
45
46 831 101, 118) in a fish cell line (RTG-2). Toxicol *in vitro*, 25:1045-1052, DOI: 10.1016/j.tiv.2011.04.004.

47 832
48
49 833 Martin-Ruiz C. M., Baird D., Roger L., Boukamp P., Krunic D., Cawthon R., Dokter M. M., van der Harst
50
51 834 P., Bekaert S., de Meyer T., Roos G., Svenson U., Codd V., Samani N. J., McGlynn L., Shiels P. G., Pooley
52
53 835 K. A., Dunning A. M., Cooper R., Wong A., Kingston A., von Zglinicki T. (2015). Reproducibility of
54
55 836 telomere length assessment: an international collaborative study. Int J Epidemiol 44: 1673-83, DOI:
56
57 837 10.1093/ije/dyu191.

58 838

839 Mazéas O. and Budzinski H. (2005). Solid-phase extraction and purification for the quantification of
1 840 polycyclic aromatic hydrocarbon metabolites in fish bile. *Anal Bioanal Chem* 383:985-990,
2
3 841 DOI: 10.1007/s00216-005-0096-4.
4
5 842
6
7 843 McLennan D., Armstrong J. D., Stewart D. C., Mckelvey S., Boner W., Monaghan P., Metcalfe N. B.
8
9 844 (2017). Shorter juvenile telomere length is associated with higher survival to spawning in migratory
10 845 Atlantic salmon. *Funct Ecol* 31:2070–2079, DOI: 10.1111/1365-2435.12939.
11
12 846
13
14 847 McLennan D., Armstrong J. D., Stewart D. C., Mckelvey S., Boner W., Monaghan P., Metcalfe N. B.
15
16 848 (2018). Telomere elongation during early development is independent of environmental temperatures
17 849 in Atlantic salmon. *J Exp Biol* 221: jeb178616, DOI: 10.1242/jeb.178616.
18
19 850
20
21 851 McChesney P. A., Elmore L. W., Holt S. E. (2005). Vertebrate Marine Species as Model Systems for
22 852 Studying Telomeres and Telomerase. *Zebrafish* 1: 349-355, DOI: 10.1089/zeb.2005.1.349.
23
24 853
25
26 854 Molbert N., Angelier F., Alliot F., Ribout C., Goutte A. (2021). Fish from urban rivers and with high
27 855 pollutant levels have shorter telomeres. *Biology Letters* 17: 20200819-20200819 , DOI:
28 856 10.1098/rsbl.2020.0819
29
30
31 857
32
33 858 Møller P., Wils R. S., Jensen D. M., Andersen M. H. G., Roursgaard M. (2018). Telomere dynamics and
34 859 cellular senescence: an emerging field in environmental and occupational toxicology. *Crit Rev Toxicol*
35 860 48: 767-788, DOI: 10.1080/10408444.2018.1538201.
36
37
38 861
39
40 862 Monaghan P., Eisenberg D. T. A., Harrington L., Nussey D. (2018). Understanding diversity in telomere
41 863 dynamics. *Philos Trans R Soc Lond B Biol Sci* 373: 20160435, DOI: 10.1098/rstb.2016.0435.
42
43 864
44
45 865 Monaghan P. and Ozanne S. E. (2018). Somatic growth and telomere dynamics in vertebrates:
46 866 Relationships, mechanisms and consequences. *Philos Trans R Soc Lond B Biol Sci* 373: 20160446, DOI:
47 867 10.1098/rstb.2016.0446.
48
49
50 868
51
52 869 Montpetit A., Alhareeri A., Montpetit M., Starkweather A., Elmore L., Filler K., Mohanraj L., Burton C.,
53 870 Menzies V., Lyon D., Jackson-Cook C. (2014). Telomere length: a review of methods for measurement.
54 871 *Nurs Res* 63: 289–299, DOI: 10.1097/NNR.0000000000000037.
55
56
57 872
58
59
60
61
62
63
64
65

873 Morinha F., Magalhães P., Blanco G. (2020). Standard guidelines for the publication of telomere qPCR
1 874 results in evolutionary ecology. *Mol Ecol Res* 20: 635-648, DOI: 10.1111/1755-0998.13152.
2
3 875
4
5 876 Munschy C., Vigneau E., Bely N., Héas-Moisan K., Olivier N., Pollono C., Hollanda S., Bodin N. (2020a).
6
7 877 Legacy and emerging organic contaminants: levels and profiles in top predator fish from the western
8
9 878 Indian Ocean in relation to their trophic ecology. *Environ Res* 188 :109761, DOI:
10 879 10.1016/j.envres.2020.109761.
11
12 880
13
14 881 Munschy C., Bely N., Héas-Moisan K., Olivier N., Pollono C., Hollanda S., Bodin N. (2020b). Tissue-
15
16 882 specific bioaccumulation of a wide range of legacy and emerging persistent organic contaminants in
17
18 883 swordfish (*Xiphias gladius*) from Seychelles, Western Indian Ocean. *Mar Pollut Bull* 158: 111436, DOI:
19 884 10.1016/j.marpolbul.2020.111436.
20
21 885
22
23 886 Ng C. Y. and Amini F. (2020). Telomere length alterations in occupational toxicants exposure: an
24
25 887 integrated review of the literature. *Expo Health*, DOI: 10.1007/s12403-020-00367-4.
26 888
27
28 889 O’Callaghan N. J., Dhillon V. S., Thomas P., Fenech M. (2008). A quantitative real-time PCR method for
29
30 890 absolute telomere length. *Biotechniques* 44: 807-809, DOI: 10.2144/000112761.
31
32 891
33
34 892 Ocalewicz K. (2013). Telomeres in Fishes. *Cytogenet Genome Res* 141: 114-125, DOI:
35 893 10.1159/000354278. DOI 10.1159/000354278.
36
37 894
38
39 895 Panfili J., De Pontual H., Troadec H., Wrigh P. J. (2002). Manual of fish sclerochronology. Ifremer/IRD
40
41 896 Coedition, Brest, France.
42 897
43
44 898 Pauliny A., Devlin R. H., Johnsson J. I., Blomqvist D. (2015). Rapid growth accelerates telomere attrition
45
46 899 in a transgenic fish. *BMC Evol Biol*, 15:159, DOI: 10.1186/s12862-015-0436-8.
47 900
48
49 901 Peterson D. R., Oi Lam Mok H., Wai Ting Au D. (2015). Modulation of telomerase activity in fish muscle
50
51 902 by biological and environmental factors. *Comp Biochem Physiol C Toxicol Pharmacol* 178: 51-59, DOI:
52 903 10.1016/j.cbpc.2015.09.004.
53 904
54
55 905 Pflaff M. W. (2004). Quantification strategies in real-time PCR. In S.A Bustin (Ed.), A-Z of quantitative
56
57 906 PCR, pp. 87–120. La Jolla, CA: IUL Biotechnology Series, International University Line.
58
59 907
60
61
62
63
64
65

908 Remen M., Nederlof M. A. J., Folkedal O., Thorsheim G., Sitjà-Bobadilla A., Pérez-Sánchez J., Oppedal
1 909 F., Olsen R. E. (2015). Effect of temperature on the metabolism, behaviour and oxygen requirements
2 of *Sparus aurata*. *Aquacult Environ Interact*, 7:115-123, DOI 10.3354/aei00141.
3 910
4 911
5 912 Saygun S (2015). The first karyological description of European Flounder, *Platichthys flesus luscus*
6
7 913 (Pallas, 1814) (Pisces, Pleuronectiformes) living in the Black Sea. *EgeJFAS*, 32: 9-14, DOI:
8 914 10.12714/egejfas.2015.32.1.02.
9 915
10 916 Sebastiano M., Angelier F., Blévin P., Ribout C., Sagerup K., Descamps S., Herzke D., Moe B., Barbraud
11 917 C., Bustnes J. O., Gabrielsen G. W., Chastel O. (2020). Exposure to PFAS is Associated with Telomere
12 918 Length Dynamics and Demographic Responses of an Arctic Top Predator. *Env Sci Tech Article ASAP*
13 919 DOI: 10.1021/acs.est.0c03099.
14 920
15 921 Sharma P., Chadha P., Singh Saini H. (2018). Tetrabromobisphenol A induced oxidative stress and
16 922 genotoxicity in fish *Channa punctatus*. *Drug Chem Toxicol* 42: 559-564, DOI:
17 923 10.1080/01480545.2018.1441864.
18 924
19 925 Simide R., Angelier F., Gaillard S., Stier A. (2016). Age and Heat Stress as Determinants of Telomere
20 926 Length in a Long-Lived Fish, the Siberian Sturgeon. *Physiol Biochem Zool* 89: 441-447, DOI:
21 927 10.1086/687378.
22 928
23 929 Suhareva, N., Aigars, J., Poikane, R., & Jansons, M. (2020). Development of fish age normalization
24 930 technique for pollution assessment of marine ecosystem, based on concentrations of mercury, copper,
25 931 and zinc in dorsal muscles of fish. *Environ Monit Assess*, 5: 192-279, DOI: 10.1007/s10661-020-08261-
26 932 x.
27 933
28 934 Tappin, A. D., and Millward, G. E. (2015). The English Channel: Contamination status of its transitional
29 935 and coastal waters. *Mar Pollut Bull*, 95: 529–550, DOI: 10.1016/j.marpolbul.2014.12.012.
30 936
31 937 Lai T-P., Wright W. E., Shay J. W. (2018). Comparison of telomere length measurement methods. *Phil*
32 938 *Trans R Soc B* 373: 20160451, DOI: 10.1098/rstb.2016.0451.
33 939
34 940 U.S. Environmental Protection Agency (1998) Method 7473 (SW-846): Mercury in solids and solutions
35 941 by thermal decomposition, amalgamation, and atomic absorption spectrophotometry, Revision 0.
36 942
37
38
39
40
41
42
43
44
45
46
47
48
49
50
51
52
53
54
55
56
57
58
59
60
61
62
63
64
65

943 van der Hammen T. and Poos J. J. (2012). Data evaluation of data-limited stocks: dab, flounder, witch,
1 944 lemon sole, brill, turbot and horse mackerel. Institute for Marine Resources and Ecosystem Studies
2 (IMARES), Wageningen. Report No. C110/12.
3 945
4 946
5 947 Vitale, F., Worsøe Clausen L., Ní Chonchúir G. (2019) (Eds). Handbook of fish age estimation protocols
6 and validation methods. ICES Cooperative Research Report No. 346. 180 pp., DOI:
7 948 10.17895/ices.pub.5221.
8 949
9 950
10 951 Wang Y., Savage SA., Alsaggaf R., Aubert G., Dagnall G. L., Spellman S. R., Lee S. J., Hicks B., Jones K.,
11 952 Katki H. A., Gadalla S. M. (2018). Telomere length calibration from qPCR measurement: limitations of
12 current method. Cells 7: 183, DOI:10.3390/cells7110183.
13 953
14 954
15 955 Wessel N., Rousseau, S., Caisey X., Quiniou F., Akcha F. (2007). Investigating the relationship between
16 956 embryotoxic and genotoxic effects of benzo[alpha]pyrene, 17 alpha-ethinylestradiol and endosulfan
17 on *Crassostrea gigas* embryos . Aquat Toxicol 85: 133-142, DOI: 10.1016/j.aquatox.2007.08.007.
18 957
19 958
20 959 Wessel N., Le Dû-Lacoste M., Budzinski H., Burgeot T., Akcha F. (2013). UPLC MS/MS quantification of
21 960 primary metabolites of benzo[a]pyrene and fluoranthene produced in vitro by Sole (*Solea solea*) liver
22 microsomal activation, Polycycl Aromat Compd 33: 52-71, DOI: 10.1080/10406638.2012.725197.
23 961
24 962
25 963 Whittemore, Elsa Vera, Eva Martínez-Nevado, Carola Sanpera, and Maria A. Blasco (2019). Telomere
26 964 shortening rate predicts species life span. PNAS 116: 15122-15127, DOI: 10.1073/pnas.1902452116.
27 965
28 966 Xin X., Senthilkumar P. K., Schnoor J. L., Ludewig G. (2016). Effects of PCB126 and PCB153 on
29 967 telomerase activity and telomere length in undifferentiated and differentiated HL-60 cells. Environ Sci
30 968 Pollut Res Int 23: 2173–2185, DOI: 10.1007/s11356-015-5187-y.
31 969
32 970 Yip B. W. P., Mok H. O. L., Peterson D. R., Wan M. T., Taniguchi Y., Ge W., Au D. W. T. (2017). Sex-
33 971 dependent telomere shortening, telomerase activity and oxidative damage in marine medaka *Oryzias*
34 972 *melastigma* during aging. Mar Pollut Bull 124: 701–709, DOI: 10.1016/j.marpolbul.2017.01.021.
35 973
36 974 Zglinicki T. (2002). Oxidative stress shortens telomeres. Trends Biochem Sci 27: 339-344, DOI:
37 975 10.1016/s0968-0004(02)02110-2.
38 976
39
40
41
42
43
44
45
46
47
48
49
50
51
52
53
54
55
56
57
58
59
60
61
62
63
64
65

977 Zhao F., Wang B., Zhang X. (2015). Induction of DNA base damage and strand breaks in peripheral
1 978 erythrocytes and the underlying mechanism in goldfish (*Carassius auratus*) exposed to
2
3 979 monocrotophos. Fish Physiol Biochem 41: 613-624, DOI: 10.1007/s10695-015-0032-2.
4

5 980

6
7 981

8
9
10
11
12
13
14
15
16
17
18
19
20
21
22
23
24
25
26
27
28
29
30
31
32
33
34
35
36
37
38
39
40
41
42
43
44
45
46
47
48
49
50
51
52
53
54
55
56
57
58
59
60
61
62
63
64
65

Table 1: Validated primer set composition and concentrations for the amplification of telomeric sequence and reference gene in flounder

Sequence/ gene	GeneBank number (NCBI)	Sens	5'-3' Sequence	Concentration nM
GAPDH	KJ510524.1	Forward	CCT-GCC-GTC-ACT-GGG-ATT-AC	500
		Reverse	ACA-GCT-CTC-CCA-CTC-TCC-TC	500
Telomere	(O'Callaghan et al., 2008)	Forward	CGG-TTT-GTT-TGG-GTT-TGG-GTT- TGGGTT-TGG-GTT-TGG-GTT	200
		Reverse	GGC-TTG-CCT-TAC-CCT-TAC-CCT- TACCCT-TAC-CCT-TAC-CCT	450

Table 2: q-PCR efficiency of the different set of primers used for the measurement of TL.

Primer set	Type of samples	Efficiency (%)	Coefficient of determination (R ²)
GAPDH	Composite flounder DNA	104	0.99
	GAPDH oligomer	99	0.99
Telomeres	Composite flounder DNA	103	0.98
	Telomere oligomer	98	0.97

Table 3: Liver metal concentrations (n=8, mean \pm standard deviation, mg kg⁻¹ dw) in flounders from Seine Estuary.

	Ag	As	Cd	Co	Cu	Fe
Liver	0.35 \pm	16.89 \pm	0.19 \pm	0.26 \pm	46.77 \pm	170.5 \pm
	0.22	5.40	0.07	0.12	10.73	66.7
	Hg	Mn	Mo	Pb	Zn	Σ
	0.13 \pm	2.98 \pm	0.31 \pm	0.09 \pm	105.3 \pm	343.9 \pm
	0.05	0.98	0.07	0.06	16.1	87.8
Muscle	Hg					
	0.270 \pm					
	0.065					

Table 4: Concentrations (ng g⁻¹ dw) of PCBs (Σ 8 congeners), DDTs (Σ 5 isomers), HCHs (Σ 3 isomers), dieldrin, PBDEs (Σ 8 congeners), PFOS and PFCAs (Σ 7 compounds with the carbon chain length > C8) in flounder muscle collected in ES (n=8, mean \pm standard deviation).

PCBs	DDTs	HCHs	Dieldrin
97.2 \pm 25.3	2.20 \pm 0.58	0.05 \pm 0.01	0.31 \pm 0.07
PBDEs	PFOS	PFCAs	
0.51 \pm 0.14	3.47 \pm 1.20	1.37 \pm 0.34	

Table 5: Correlation matrix between absolute and relative TL, DNA damage and chemical contaminant concentrations in the flounder (N= 8, R²: coefficient of determination, p value is given for $\alpha = 0.05$, underlined values are significant for $\alpha = 0.10$)

	Absolute TL		Relative TL		% Tail DNA	
	R ²	p value	R ²	p value	R ²	p value
% Tail DNA	0.167	0.315	0.305	0.156	-	-
PAH metabolites	0.070	0.525	0.235	0.223	0.217	0.245
TMEs	0.090	0.470	0.067	0.535	0.236	0.222
PCBs	0.327	0.139	0.382	<u>0.103</u>	0.199	0.268
DDT	0.374	0.107	0.423	<u>0.081</u>	0.295	0.164
HCH	0.022	0.726	0.049	0.598	0.025	0.711
Dieldrin	0.335	0.133	0.349	0.123	0.167	0.314
PFOS	0.050	0.594	0.042	0.626	0.137	0.368
PFCA	0.123	0.395	0.100	0.445	0.031	0.678
OCPs	0.368	0.111	0.414	<u>0.085</u>	0.278	0.179
PBDEs	0.184	0.290	0.219	0.242	0.186	0.286

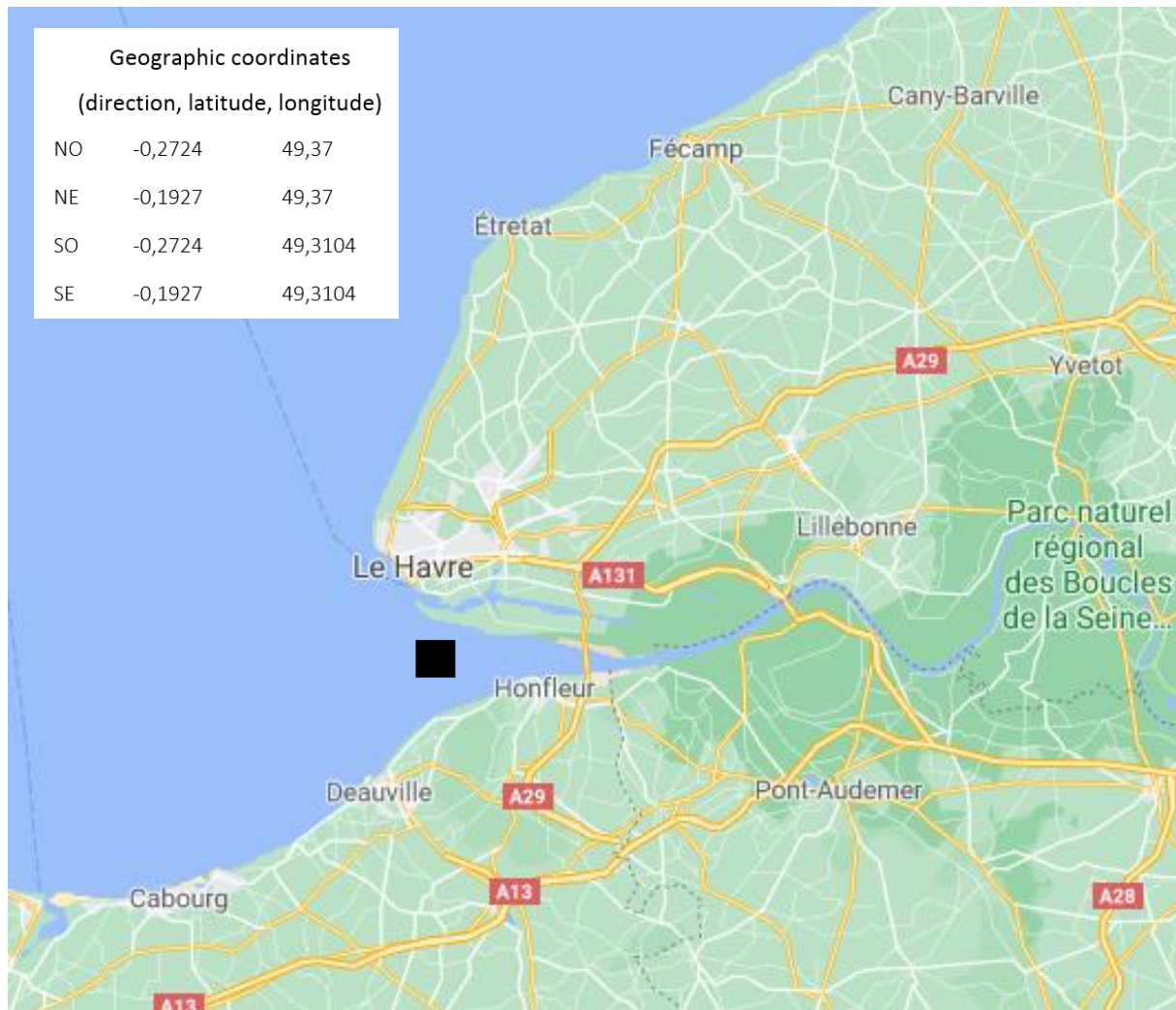


Figure 1: Localization of the sampling location in Seine Bay where flounders were caught during the SeliSeine survey (13-21 September 2018, R/V Antéa)

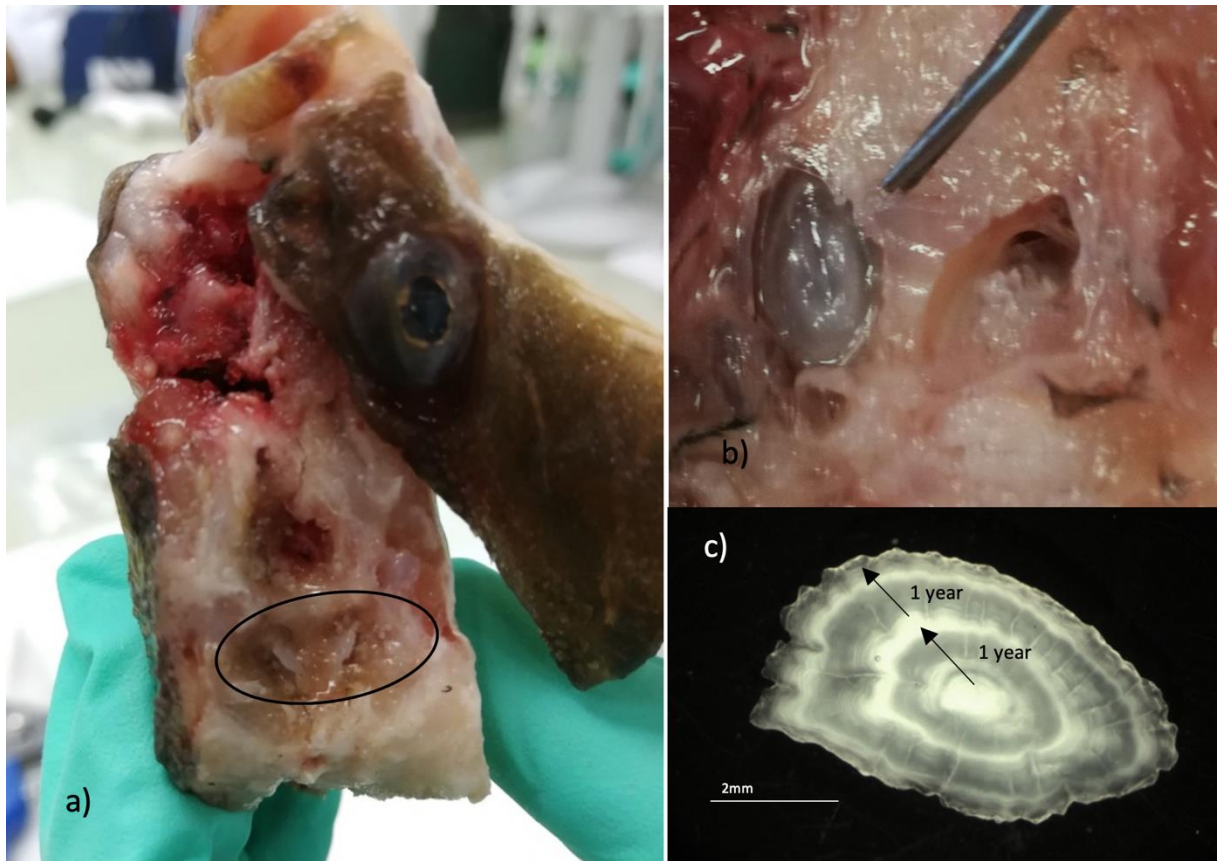


Figure 2: Sampling of flounder otoliths. After opening the skull (a), the sagittal otoliths are in the inner ear (b). The whole otolith are analysed under a microscope (c). The annual growth ring (i.e. annulus) counted on otoliths were represented by alternations of an opaque and a hyaline zone (here, a 2-year-old flounder).

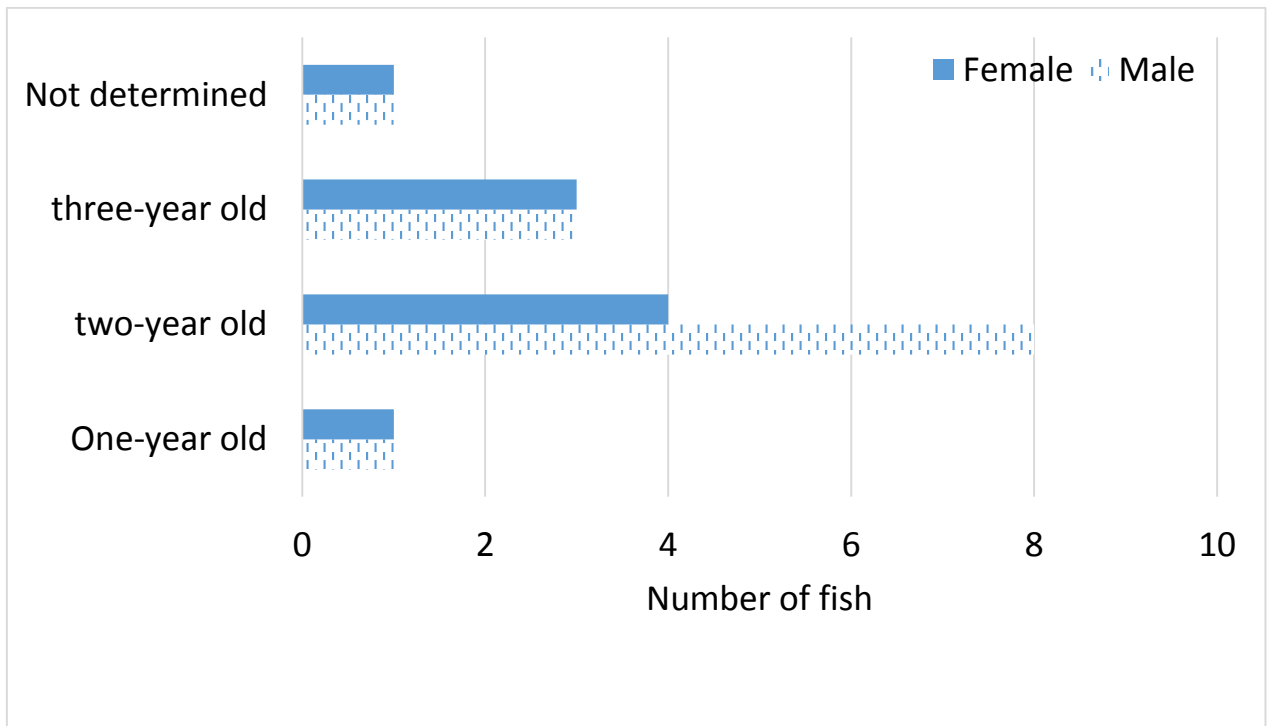


Figure 3: Number and sex of flounders caught during the survey. Not determined: the sclerochronology analysis could not be carried out because of the physical state of the otoliths being either broken or decalcified.

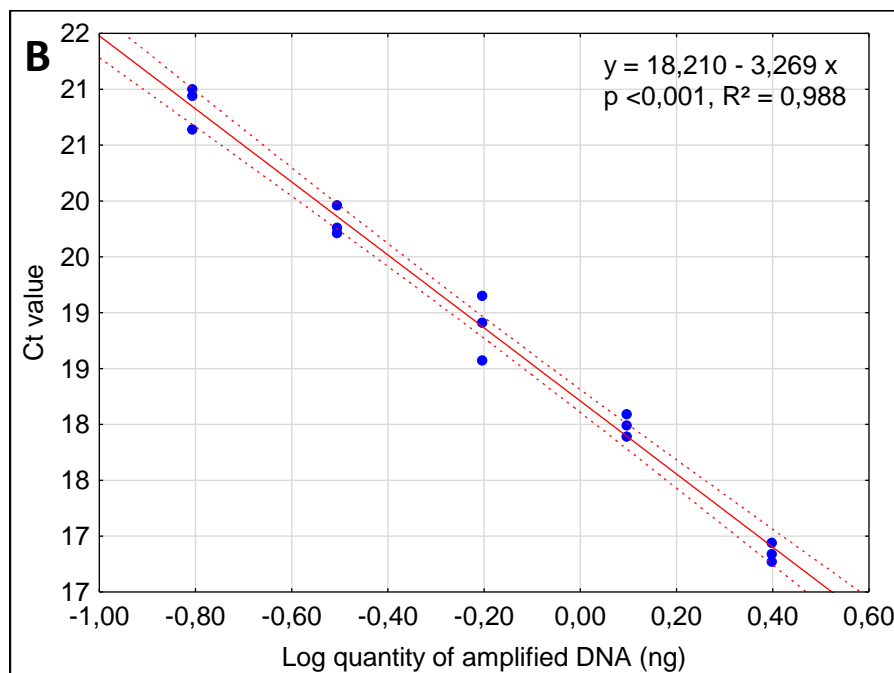
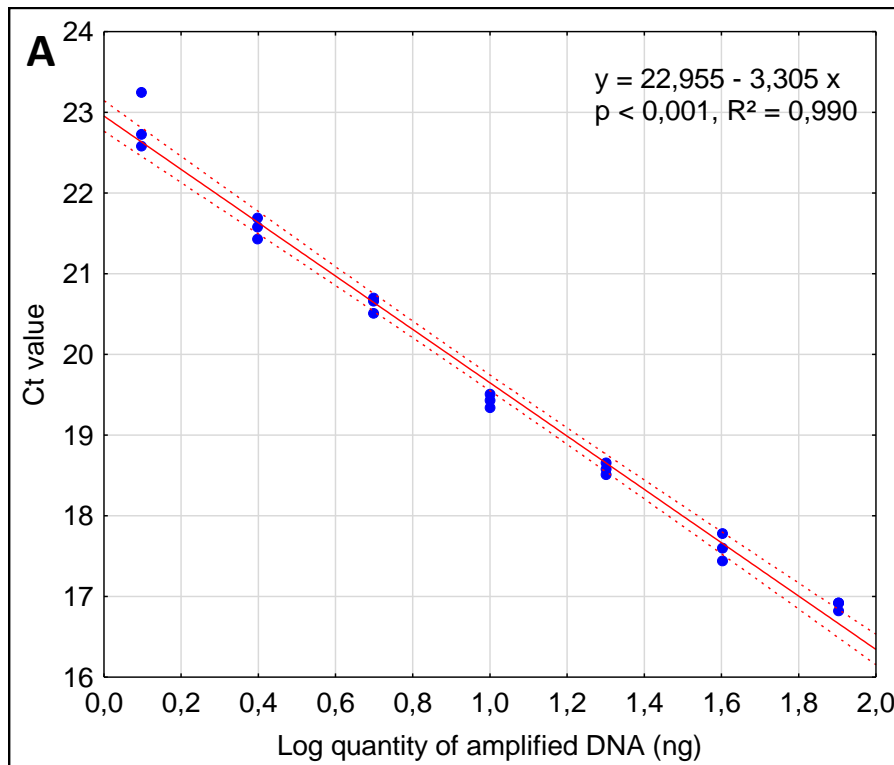


Figure 4: Validation of the q-PCR conditions by the linear relationship between amplified DNA amount and Ct values for (A) GAPDH gene and (B) telomeres. Regression bands represented the 95% confidence interval.

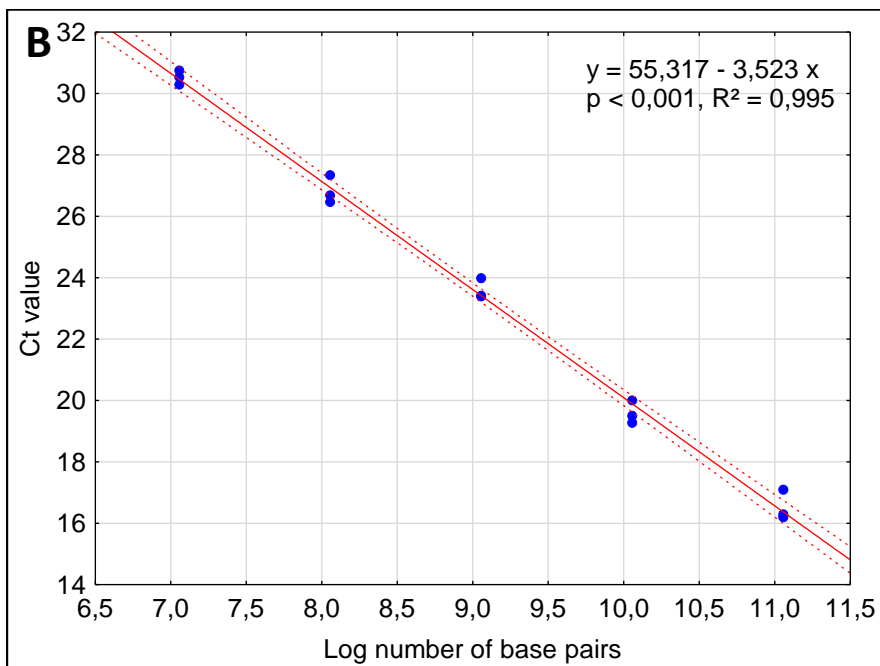
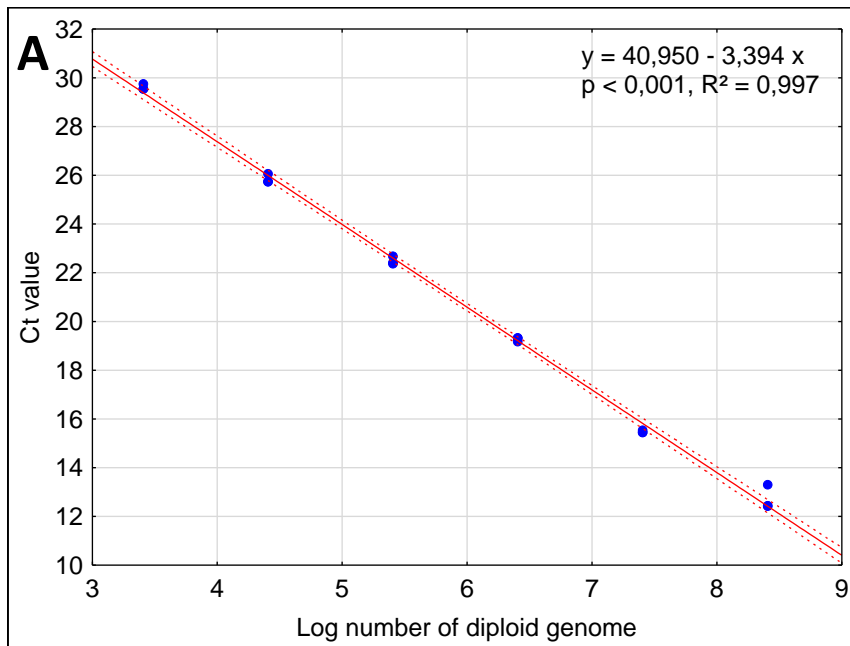


Figure 5: Calibration curve established for (A) GAPDH oligomer and (B) telomeric oligomer. For each calibration curve, plasmidic DNA was added to maintain the amount of DNA stable (1ng) in each well of the plate. Regression bands represented the 95% confidence interval.

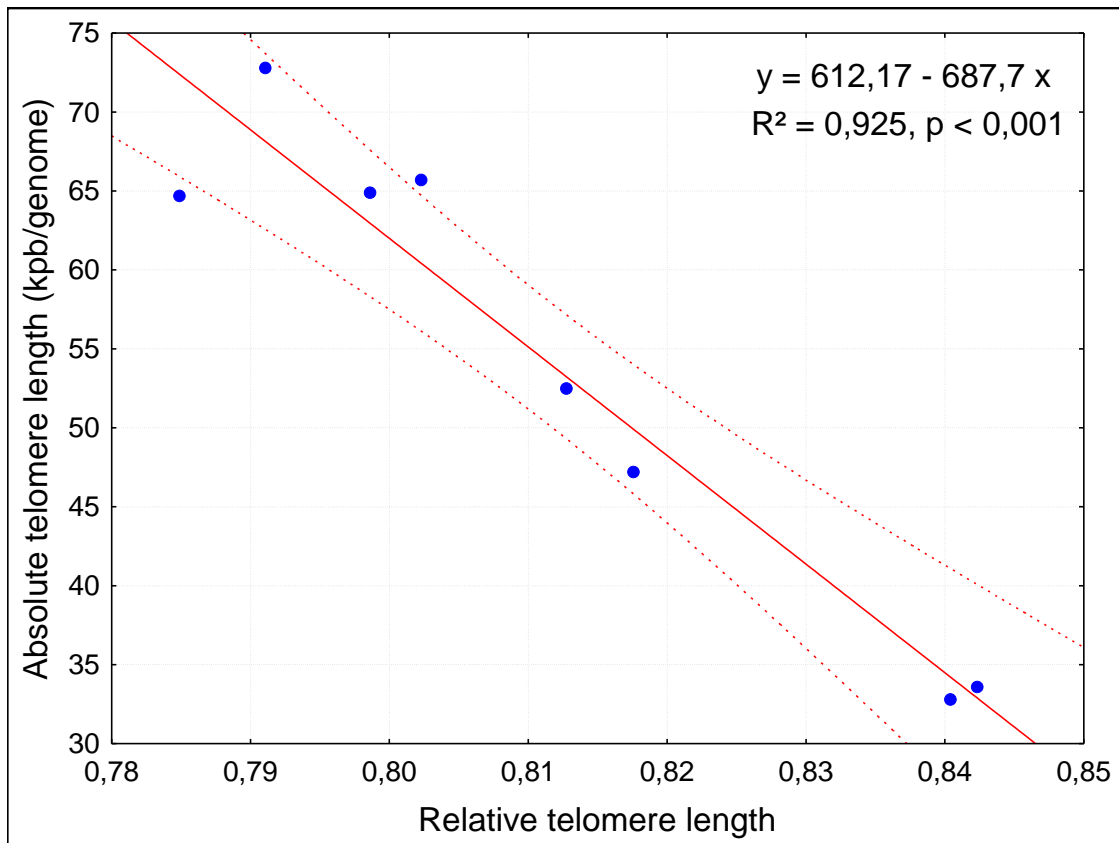


Figure 6: Correlation between absolute and relative TLs in the European flounder. Regression bands represented the 95% confidence interval.

CRedit author statement

F. Akcha: conceptualisation, methodology, writing-original draft preparation, funding acquisition, C. Cahuc: methodology, validation, J. Rouxel: methodology, C. Munsch: analysis of organic contaminants, Y. Aminot: analysis of organic contaminants, T. Chauvelon: analysis of MTEs, K. Mahe: analysis of fish otoliths, H. Budzinski: analysis of PAH metabolites, A. Mauffret: resources, funding acquisition.

Author Competing Interests

Funding Sources: Financial support for research (salaries, equipment, supplies, travel reimbursement), speaker/organizer honoraria.

Employment: Employment while engaged in this research, present or anticipated employment by any organization that may gain or lose financially through publication of this paper.

Personal Financial Interests: Stocks or shares in or ownership of companies affected by publication of this research, consulting fees/remuneration, royalties, from organizations which may profit or lose as a result of publication, patents or patent applications whose value and integrity may be affected due to publication.

Institutional Competing Interests

Are you aware that your academic institution or employment has a financial interest in or a financial conflict with the subject matter or materials discussed in this manuscript? Yes/**No**

DECLARATION OF COMPETING INTERESTS

Title of Manuscript:

Measurement of telomere length in the European flounder (*Platichthys flesus*) from the Seine Estuary: investigating a link between telomere length, DNA damage and chemical body burden

Corresponding Author:

Farida AKCHA

None declared under financial, general, and institutional competing interests. I had full access to all study data, take fully responsibility for the accuracy of the data analysis, and have authority over manuscript preparation and decisions to submit the manuscript for publication.

F. Akcha

5th January 2021

A handwritten signature in black ink, appearing to read 'F. Akcha', is written over a light grey rectangular background.